Smart Mitigation of flow-induced Acoustic Radiation and Transmission for reduced Aircraft, surface traNSport, Workplaces and wind enERgy noise

Acoustic Control with new martial technologies and their industrial perspectives

- *Determination of Non-linear scattering matrices for perforated plates using tonal, multi and random excitation*
  Niloofar Sayyad Khodashenas
- *Flow-Acoustic Interaction with Innovative Materials*
  Massimo D'Elia
- *Development of Intelligent Lightweight Material Solutions for Improved Vibro-Acoustic Transmission Problems*
  Felipe Alves Pires
- *Electroacoustic Liners and Industrial Perspectives*
  Emanuele De Bono

SmartAnswer Closure Meeting (M48) Lecture Series/Workshop/Consortium meeting ,VKI, Belgium, November 23rd-27th, 2020, Online Event

H2020 MARIE SKŁODOWSKA-CURIE ACTIONS

Introduction

Vibroacoustic metamaterial

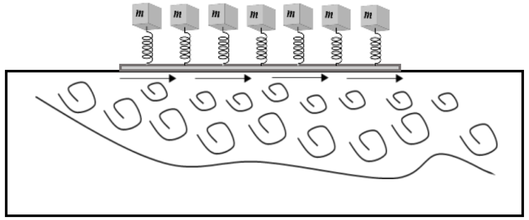

Passive Liners

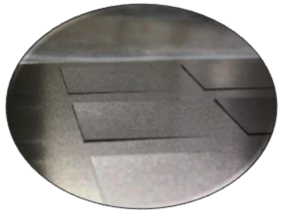

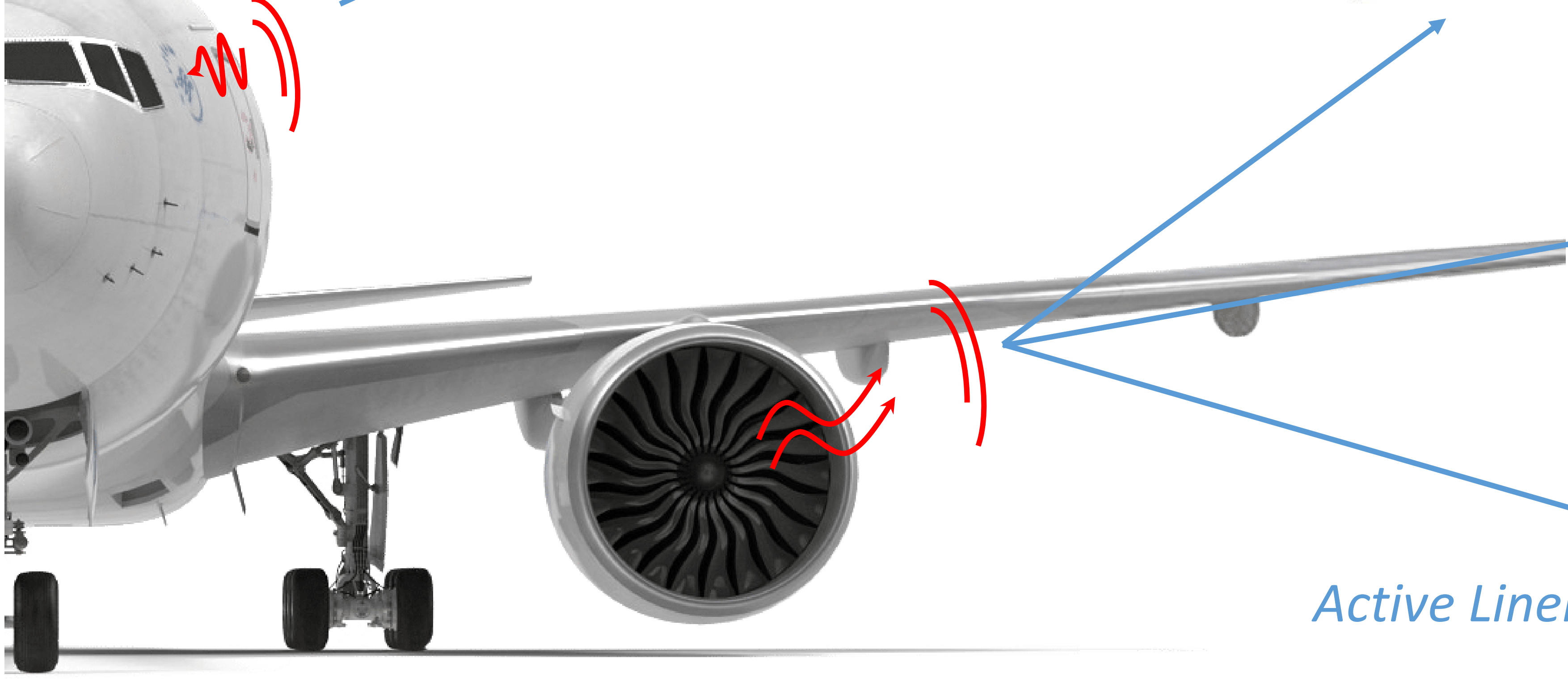

...and their nonlinearities

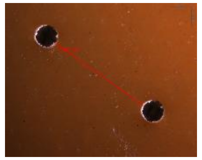

Active Liners

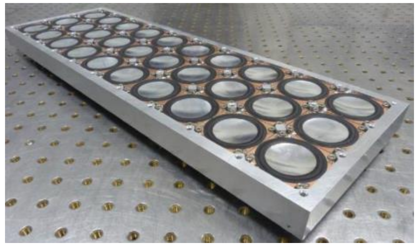

Introduction

Flow-Acoustic Interaction
with
Innovative Materials

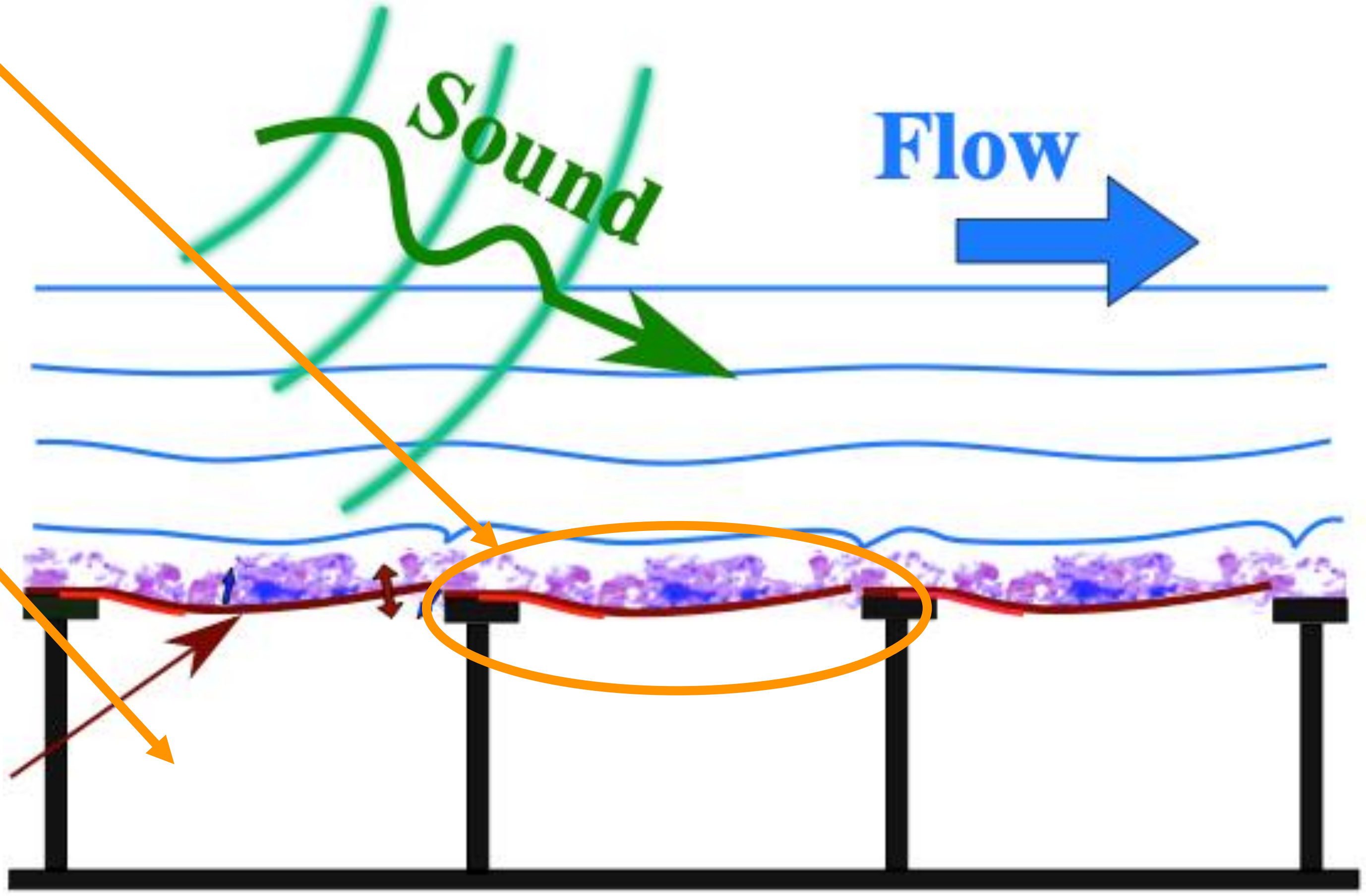

Introduction

First Step:

Flow-Acoustic Interaction

Flow-Acoustic interactions over small cavities:
Application to corrugated pipes

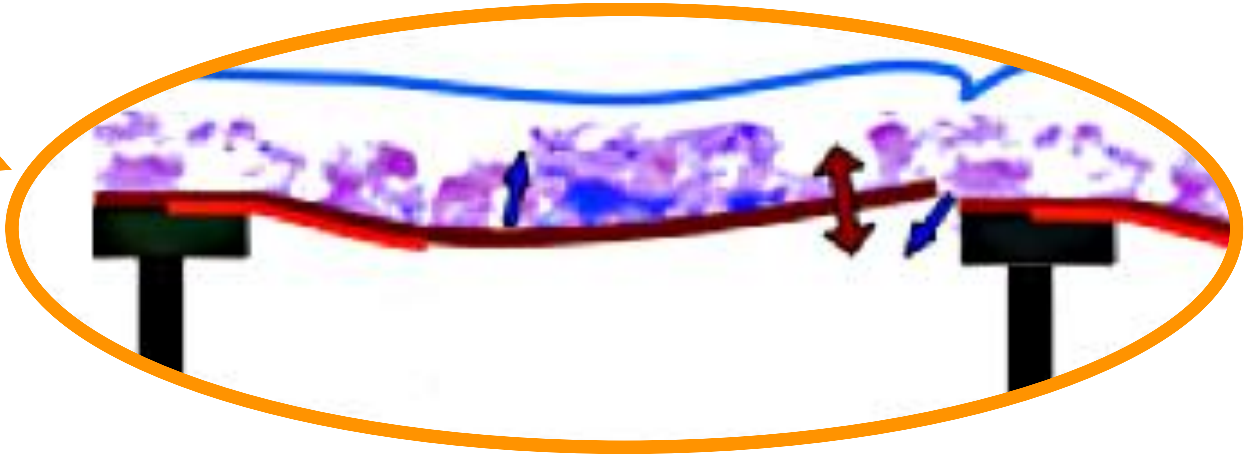

Industrial interest of TNO innovation for life

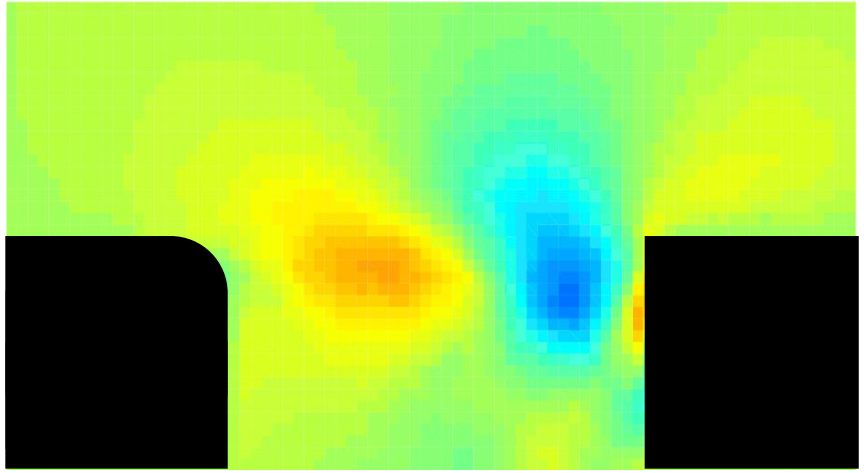

Introduction

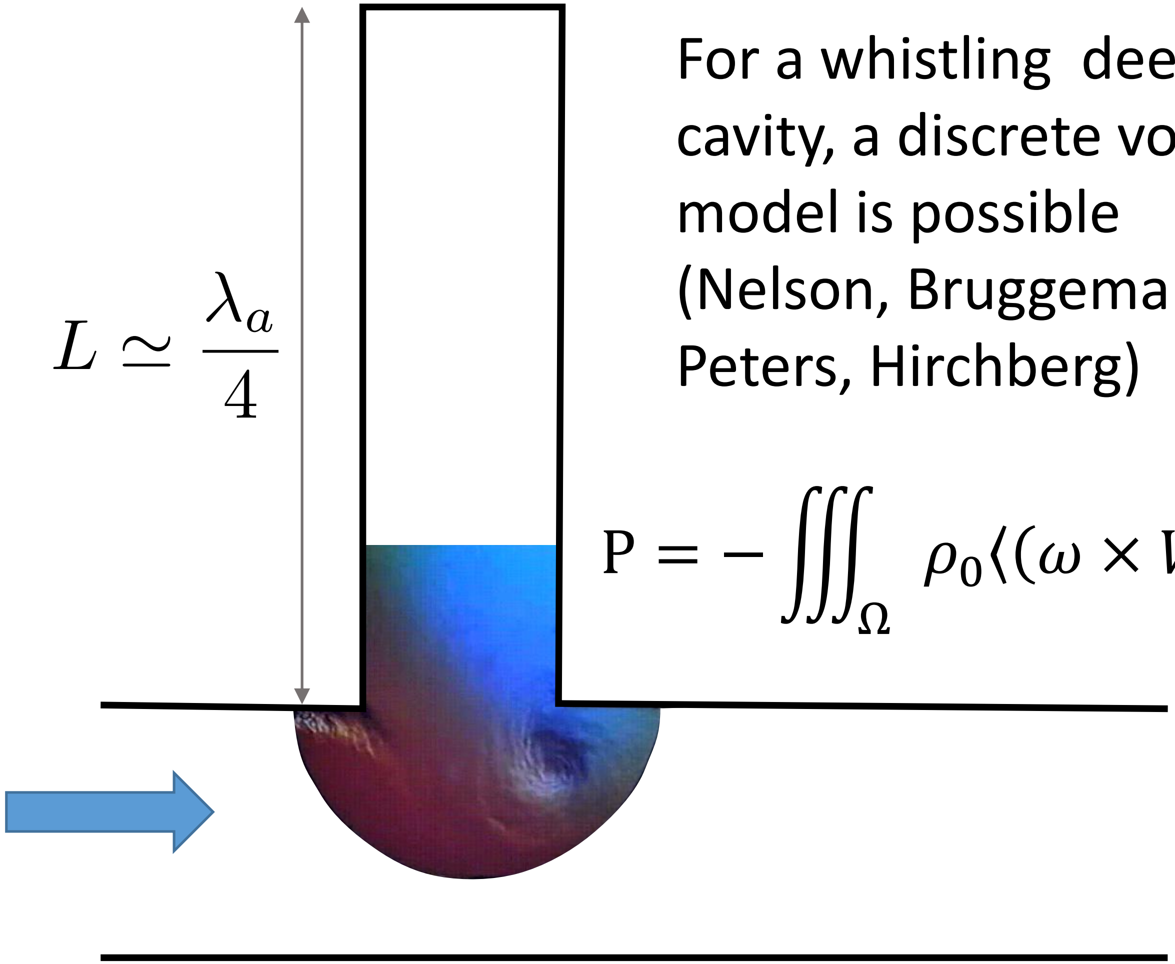

$$L \simeq \frac{\lambda_a}{4}$$

For a whistling deep cavity, a discrete vortex model is possible (Nelson, Bruggeman, Peters, Hirchberg)

$$\mathrm{P} = -\iiint_{\Omega} \rho_0 \langle(\omega \times V)\rangle \cdot u_a \, d\Omega$$

Schlieren visualization of a vortex with large sound amplitude (A.P. J. Wijnands and O. Schneider, TU Eindhoven)

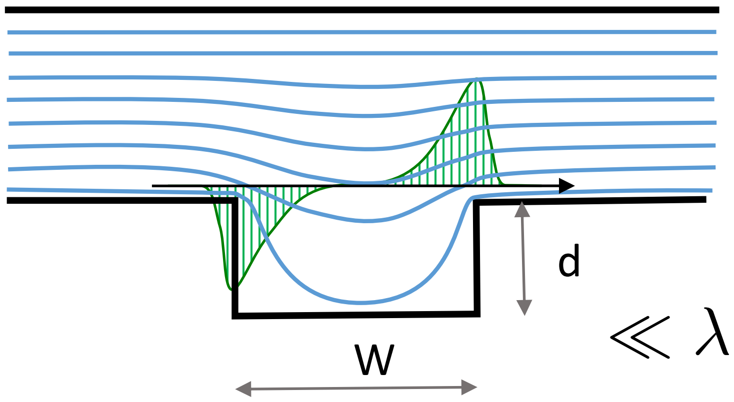

$\ll \lambda_a$

- **Is it possible to do the same with small shallow cavities?**
- **What happens just before whistling?**

Introduction

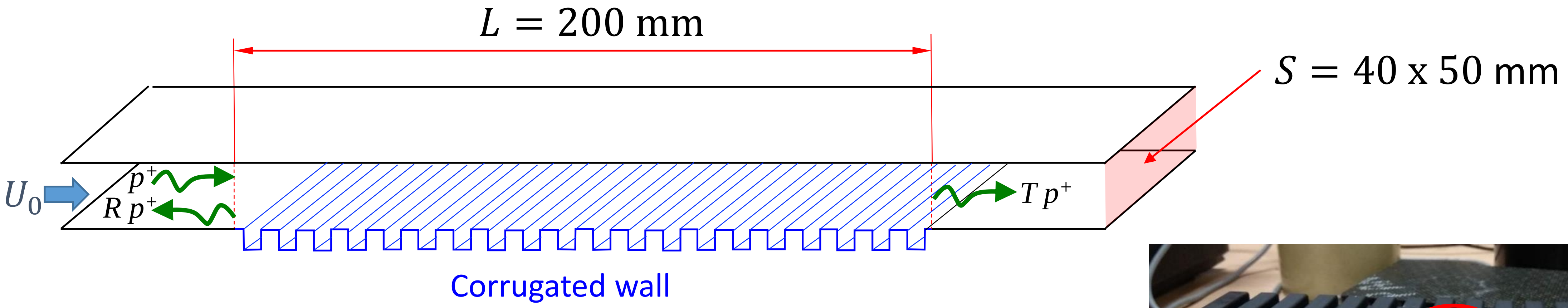

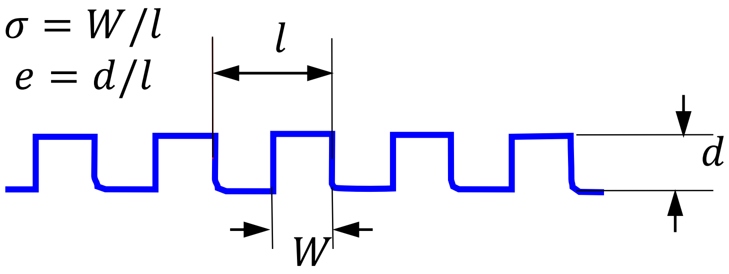

$W = 8$ mm
$d = 4$ mm, $l = 12$ mm

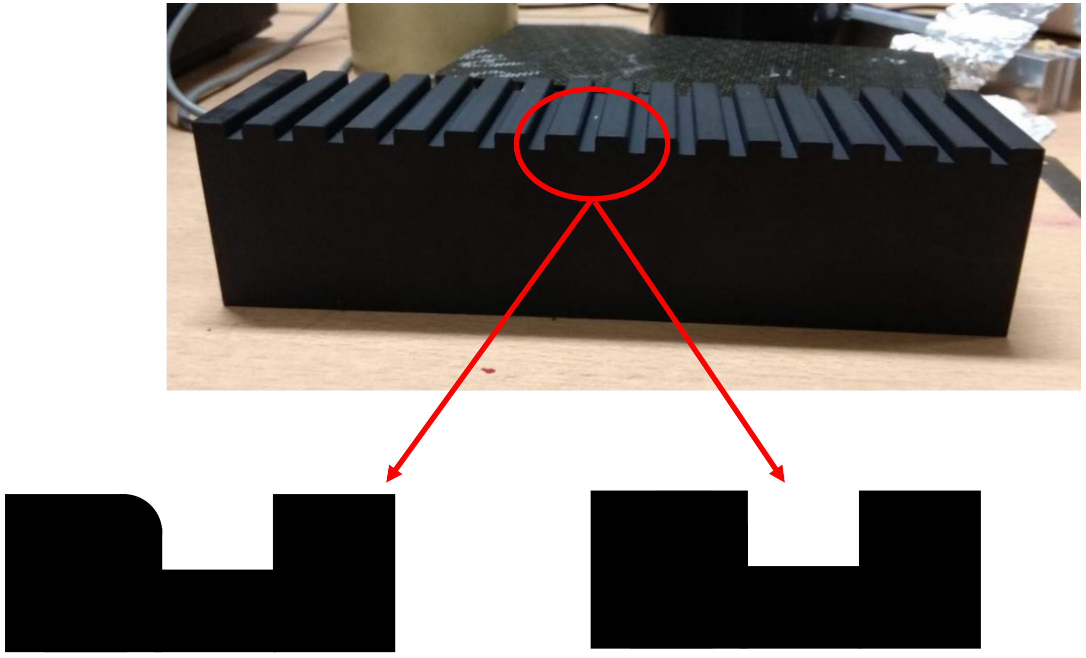

Conf. A – Round-Square Edges

Conf. B – Square-Square Edges

Introduction

Oscillations:

- Oscillations of transmission coefficients with flow
- Frequency of oscillations dependent on flow velocity: constant Sr

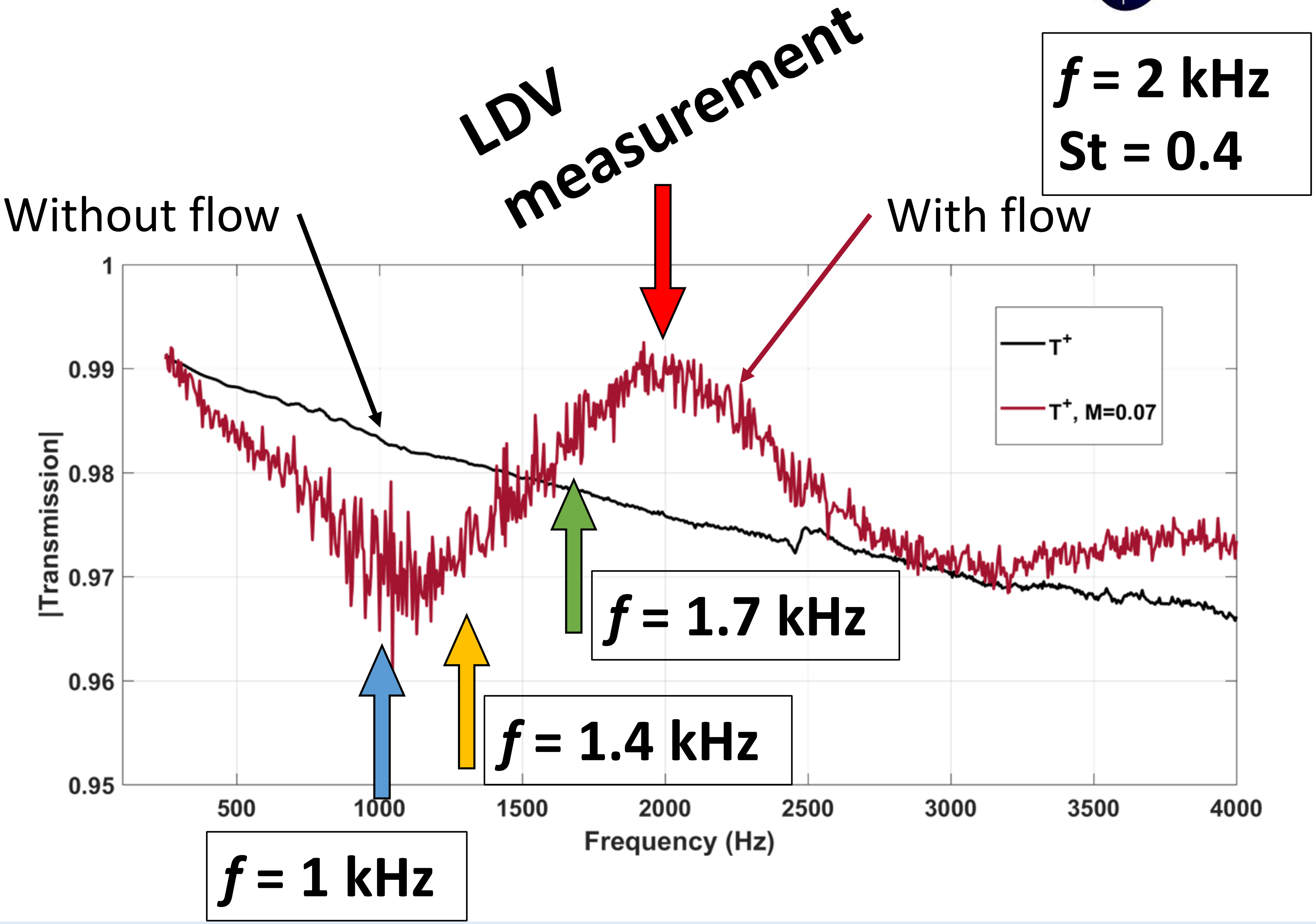

LDV Setup

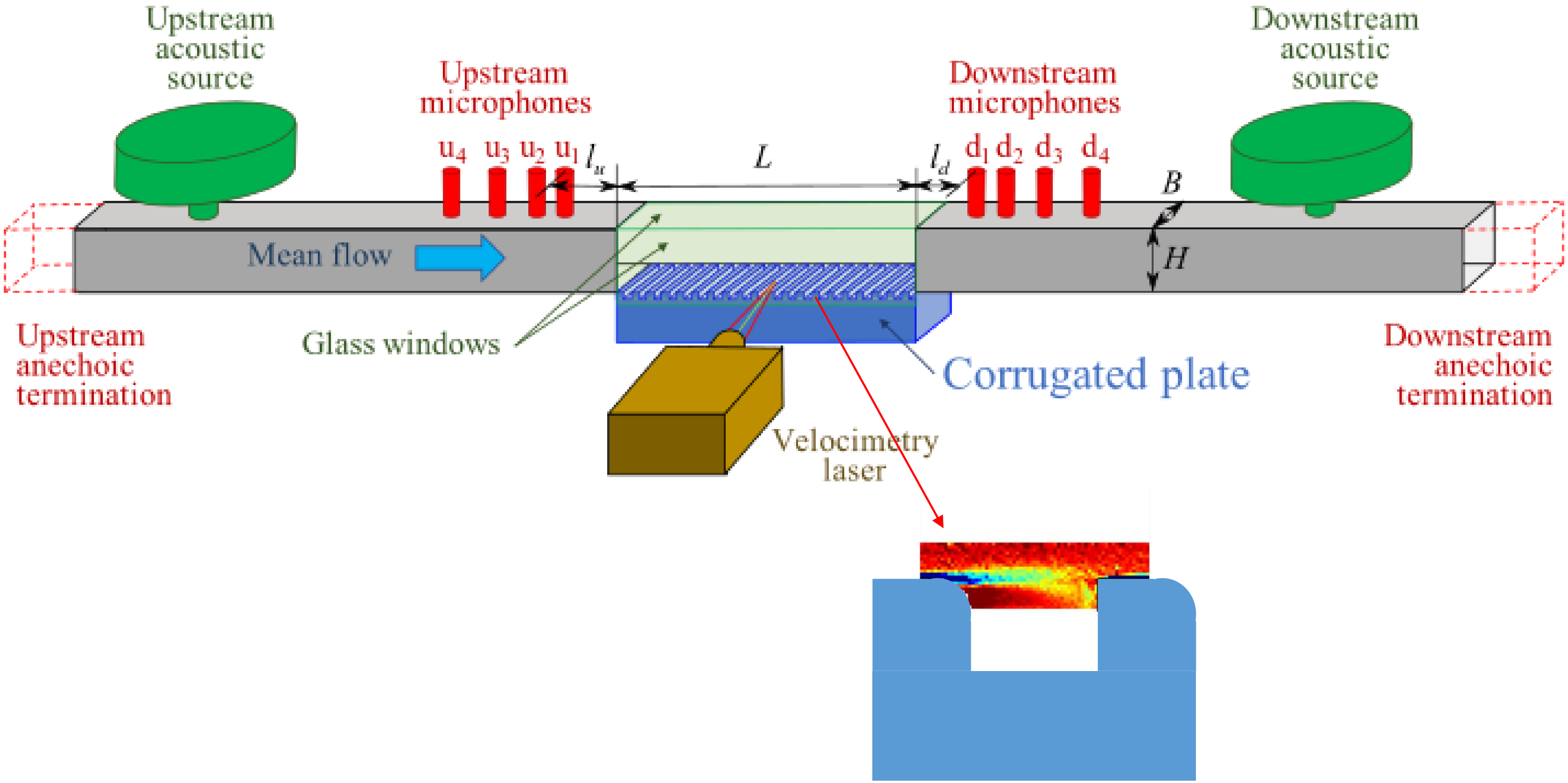
Upstream acoustic source
Upstream microphones
Downstream microphones
Downstream acoustic source
u_4 u_3 u_2 u_1 l_u
L
l_d d_1 d_2 d_3 d_4
B
H
Mean flow
Upstream anechoic termination
Glass windows
Corrugated plate
Downstream anechoic termination
Velocimetry laser

LDV Technique

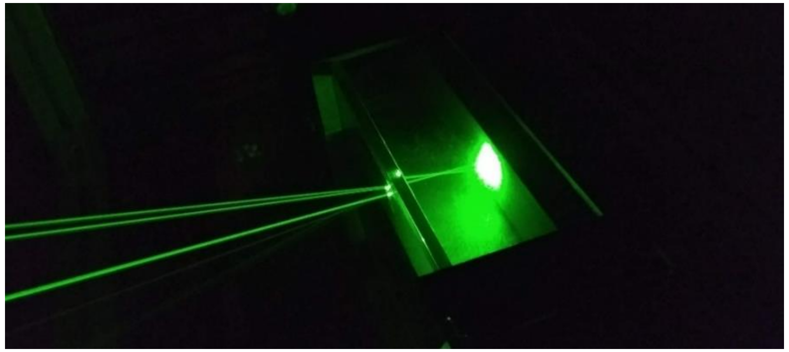

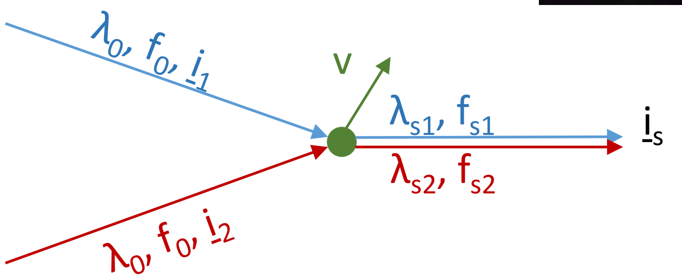

$f_{s1} = f_0 + V/\lambda_0(\underline{i}_s - \underline{i}_{s1})$
$f_{s2} = f_0 + V/\lambda_0(\underline{i}_s - \underline{i}_{s2})$

→ $\mathbf{f_D = f_{s1} - f_{s2} = V/\lambda_0(\underline{i}_{s2} - \underline{i}_{s1})}$

Retrieved velocity: $V = v_{mean} + v_f + v_t$
Sum of average, fluctuating and turbulent components

Fluctuating component can be retrieved either by phase-locked measurements or by <u>least-square approach</u> (chosen method)

Corrugated pipe - LDV Measurements

As we are interested in the vorticity shed by the cavities, we measured 1 mm inside the (fourth) cavity and around 1.3 mm above, with a step of 0.10 mm (machine resolution).

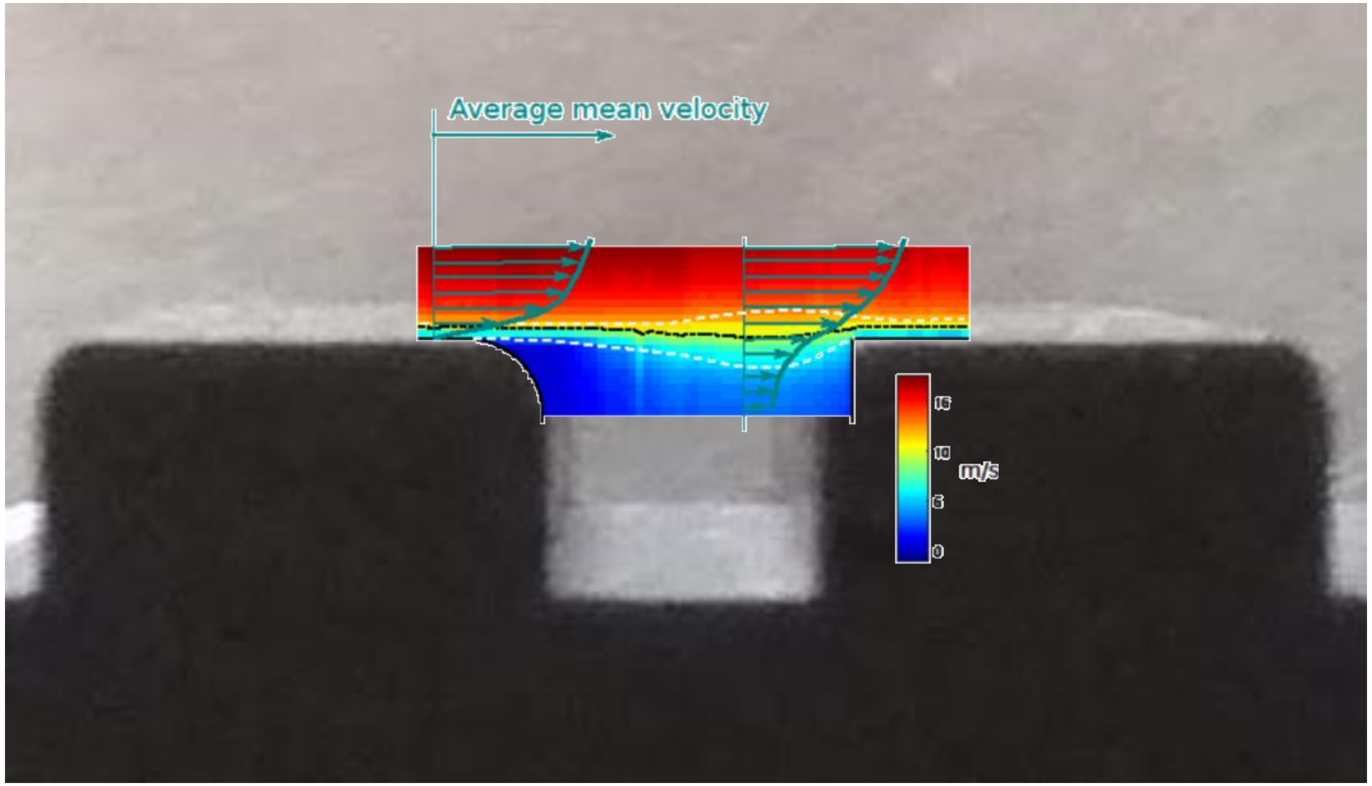

Geometrical restrictions: acquisition in two steps and tilt

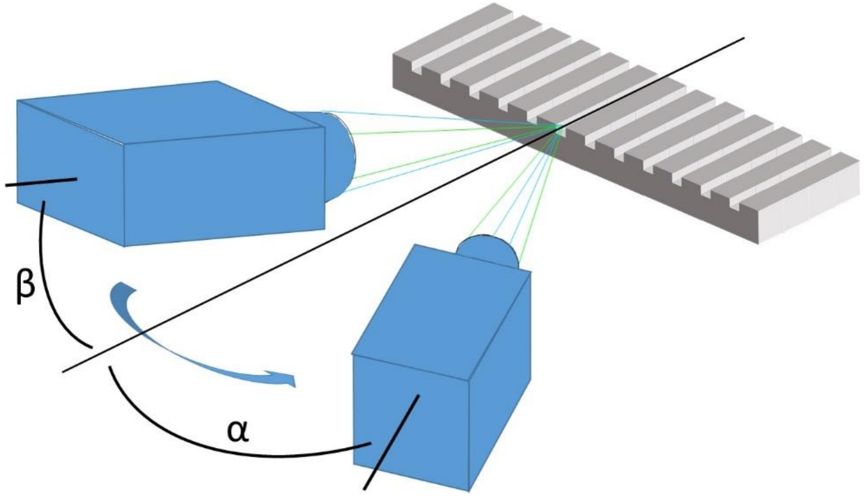

Corrugated pipe - LDV Measurements

By looking at the velocity phase right above the cavity, we can find a very clear linear behaviour.
From this, we can then obtain the shed vorticity traveling velocity, which, when traced down in black on the left figure, coincide pretty well with the vorticity core.

$$v_f = |V_f| e^{-ikW} \rightarrow \mathrm{k} = \frac{angle(v_f)}{W} \rightarrow \lambda_t = \frac{2\pi}{k}$$

$$c_t = \lambda_t f = 9.25\ m/s$$

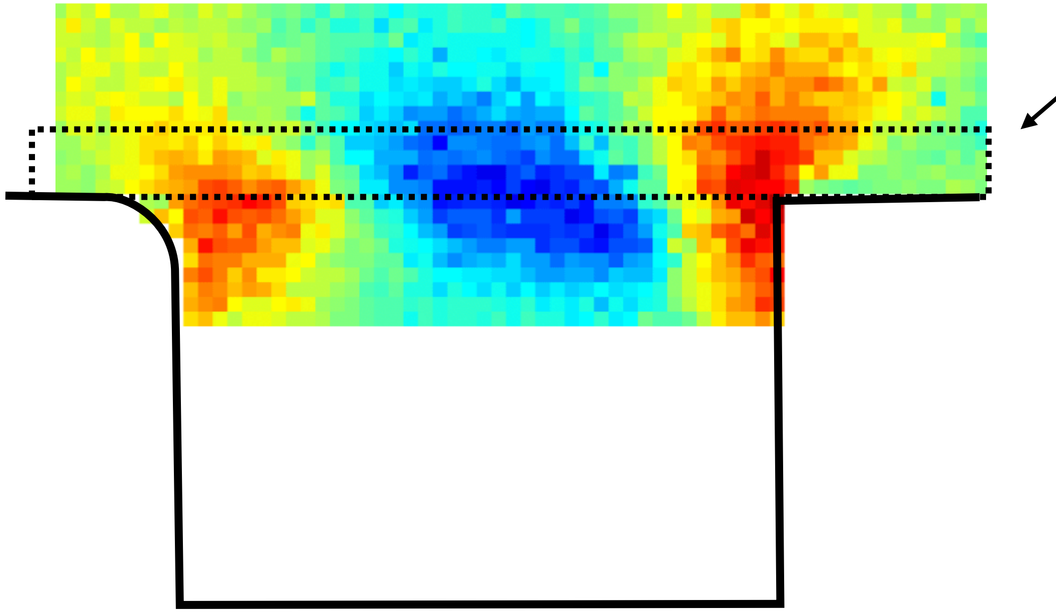

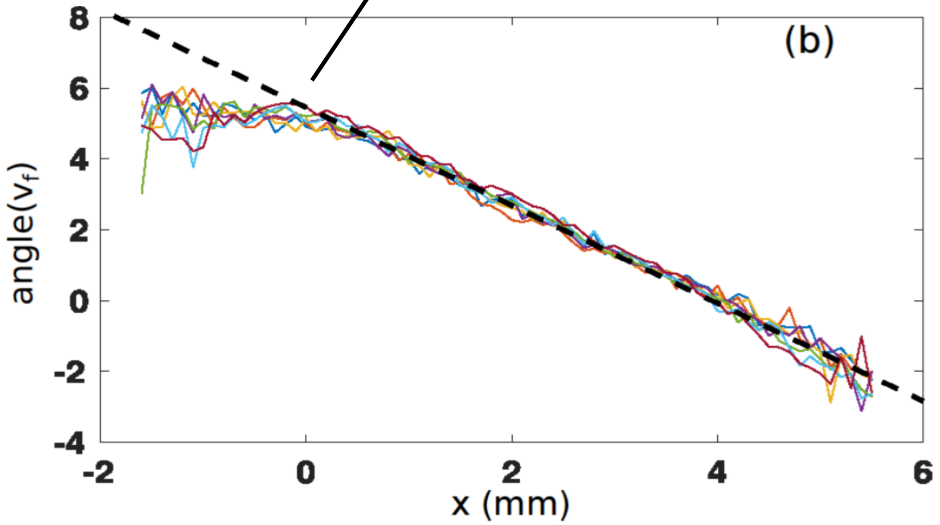

Corrugated pipe - LDV Measurements

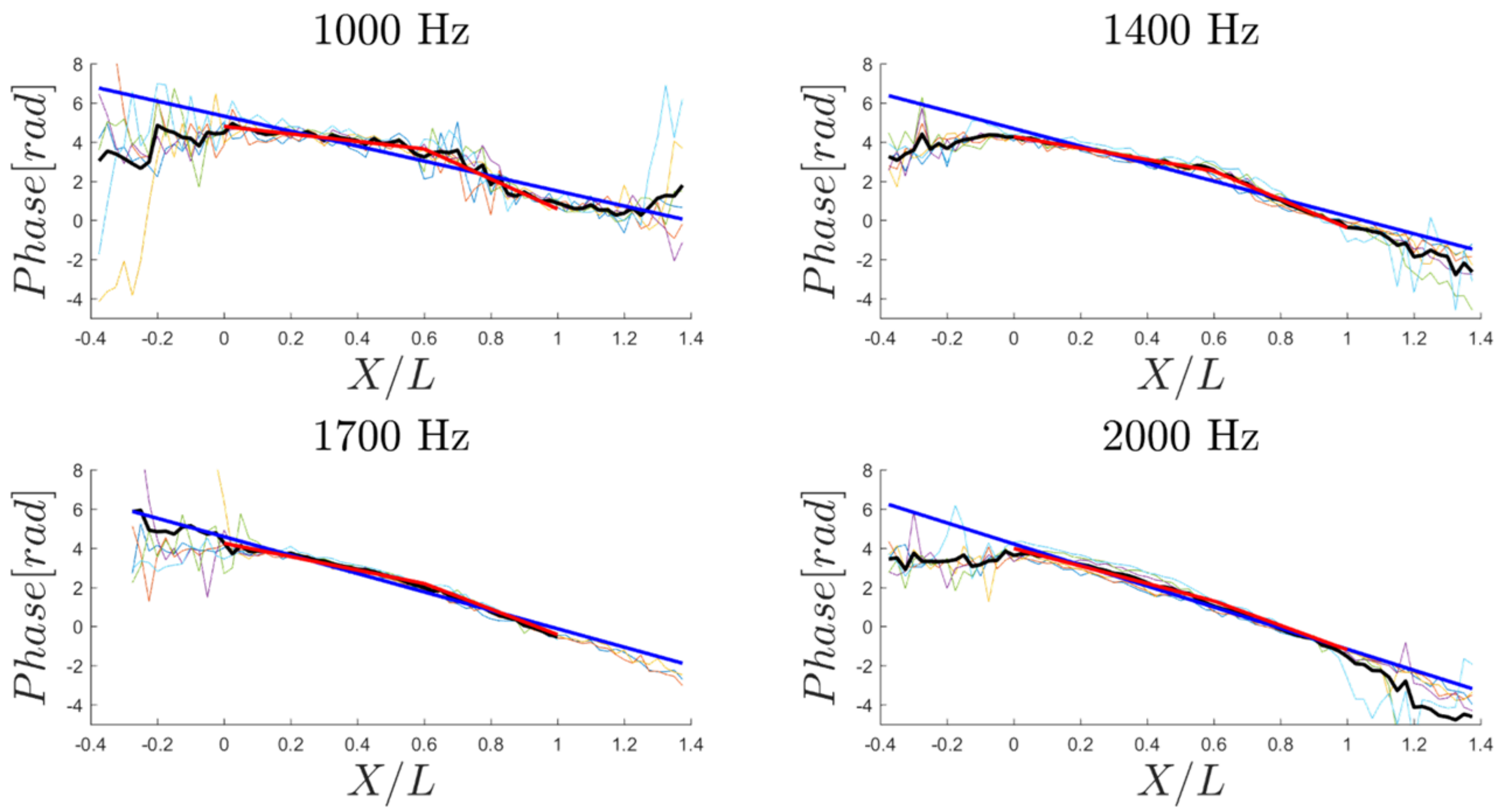

$$v_f = |V_f| e^{-ikW} \rightarrow \mathrm{k} = \frac{angle(v_f)}{W}$$

$$\rightarrow \lambda_t = \frac{2\pi}{k}$$

$c_t = \lambda_t f = \mathbf{6.58}\, m/s$, $f = 1000\ Hz$
$c_t = \lambda_t f = 7.86\, m/s$, $f = 1400\ Hz$
$c_t = \lambda_t f = 9.09\, m/s$, $f = 1700\ Hz$
$c_t = \lambda_t f = \mathbf{9.36}\, m/s$, $f = 2000\ Hz$

Transparent Layer

- In several novel metamaterial application, metamaterial are porous.

- When the field of application is extended in presence of an external flow, usually a layer able to keep out the flow but not the acoustics is imposed (and its realization often overlooked)

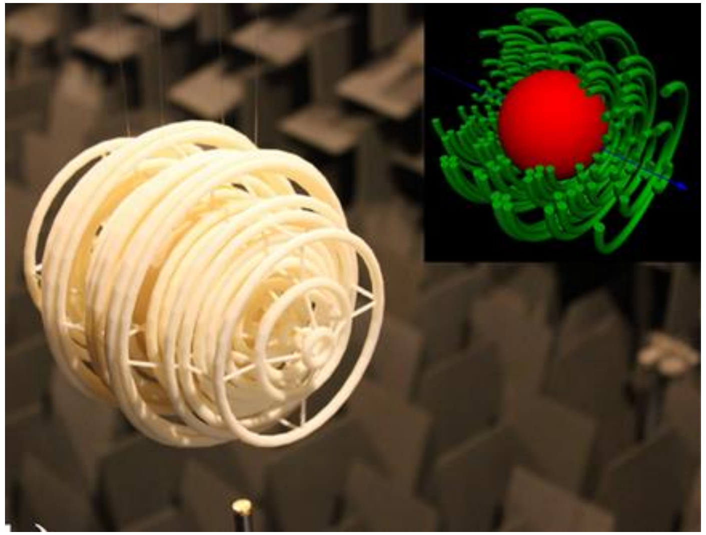

Transparent Layer

- The idea of using a Kevlar sheet is sometimes suggested since acoustically transparent walls made from tensioned Kevlar cloth are nowadays used in wind tunnels

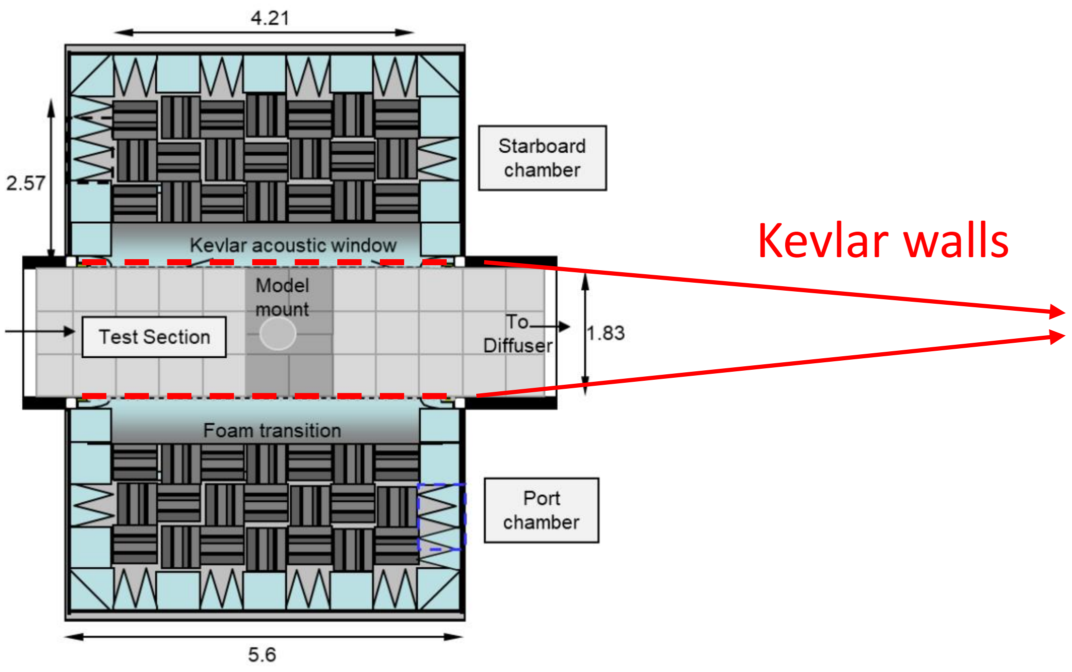

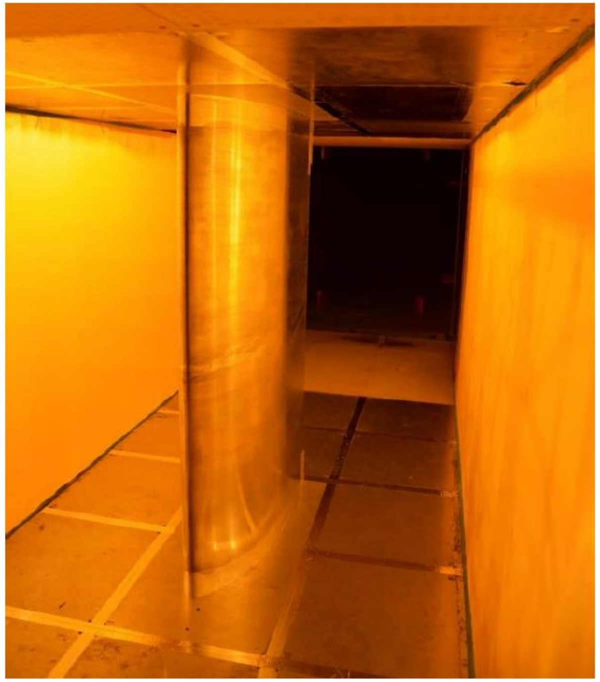

Transparent Layer

- Then, let's find out if a Kevlar sheet is fit to achieve the same results at smaller scales (i.e. of acoustic metamaterial interest)

Metamaterial :
Helmholtz resonator

without

with Kevlar

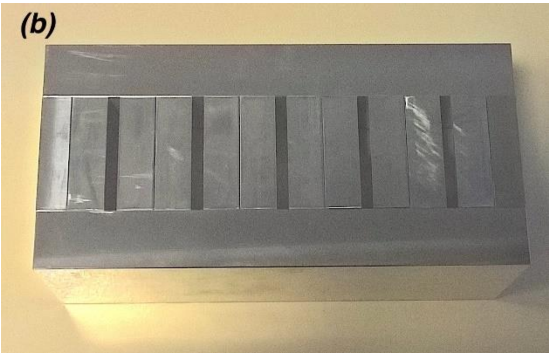

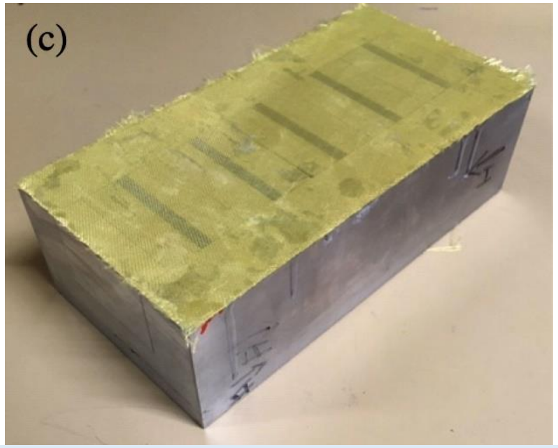

Transparent Layer

… in waveguide *with flow*

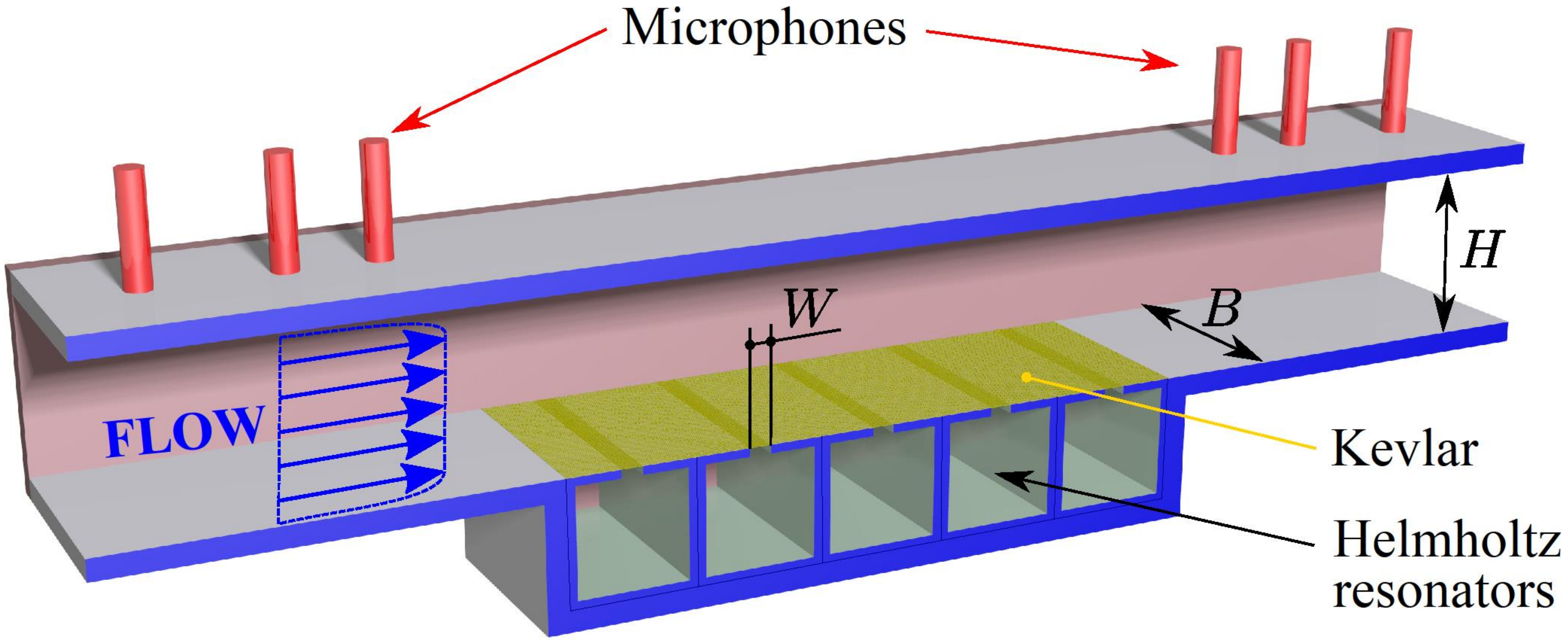

Testing: no Kevlar

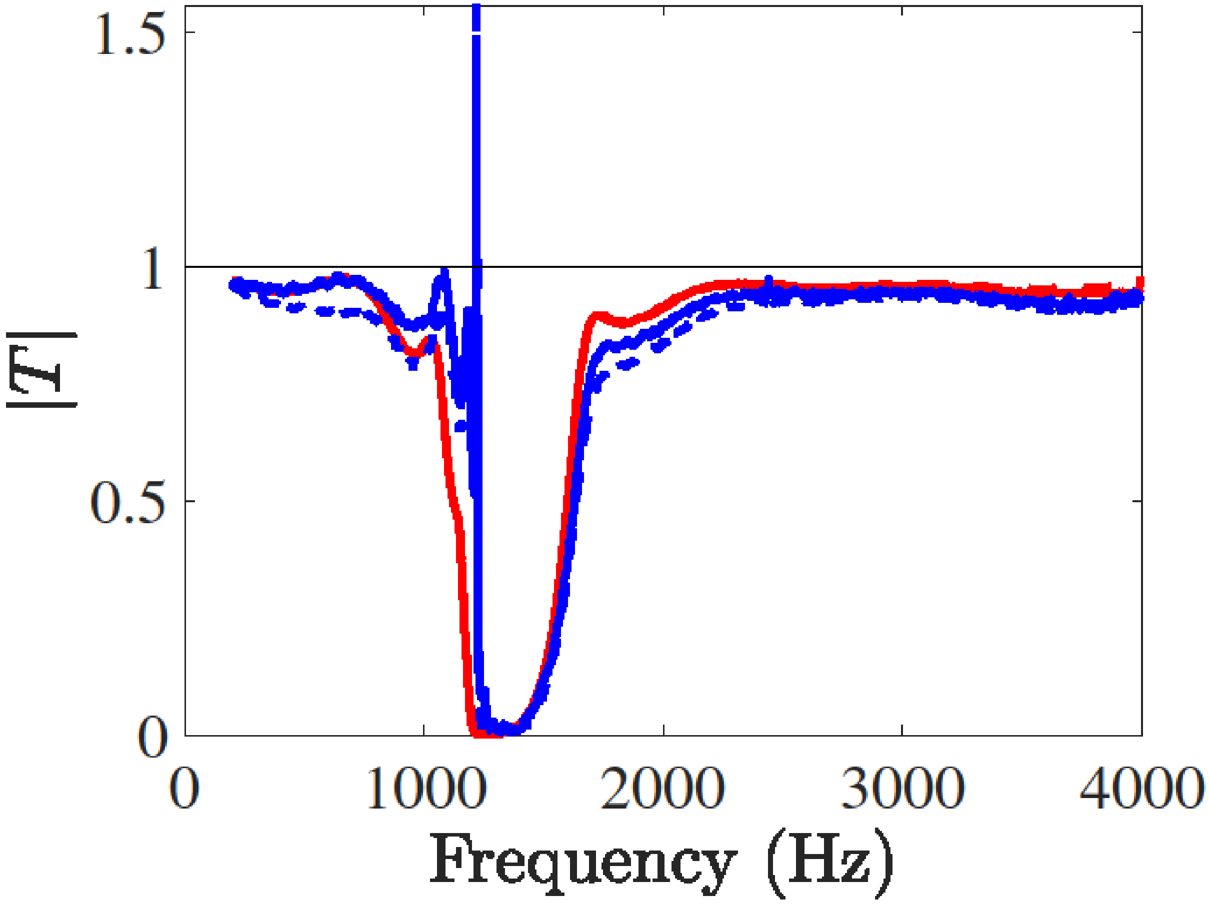

- In red, the transmission curves for the no flow, no Kevlar case. Attenuation can be seen around the characteristic frequency of the resonator
- In blue the same case, but for a M = 0.073 flow case. It is possible to appreciate a whistling (|T|>1) right above 1000 Hz

Testing: with Kevlar

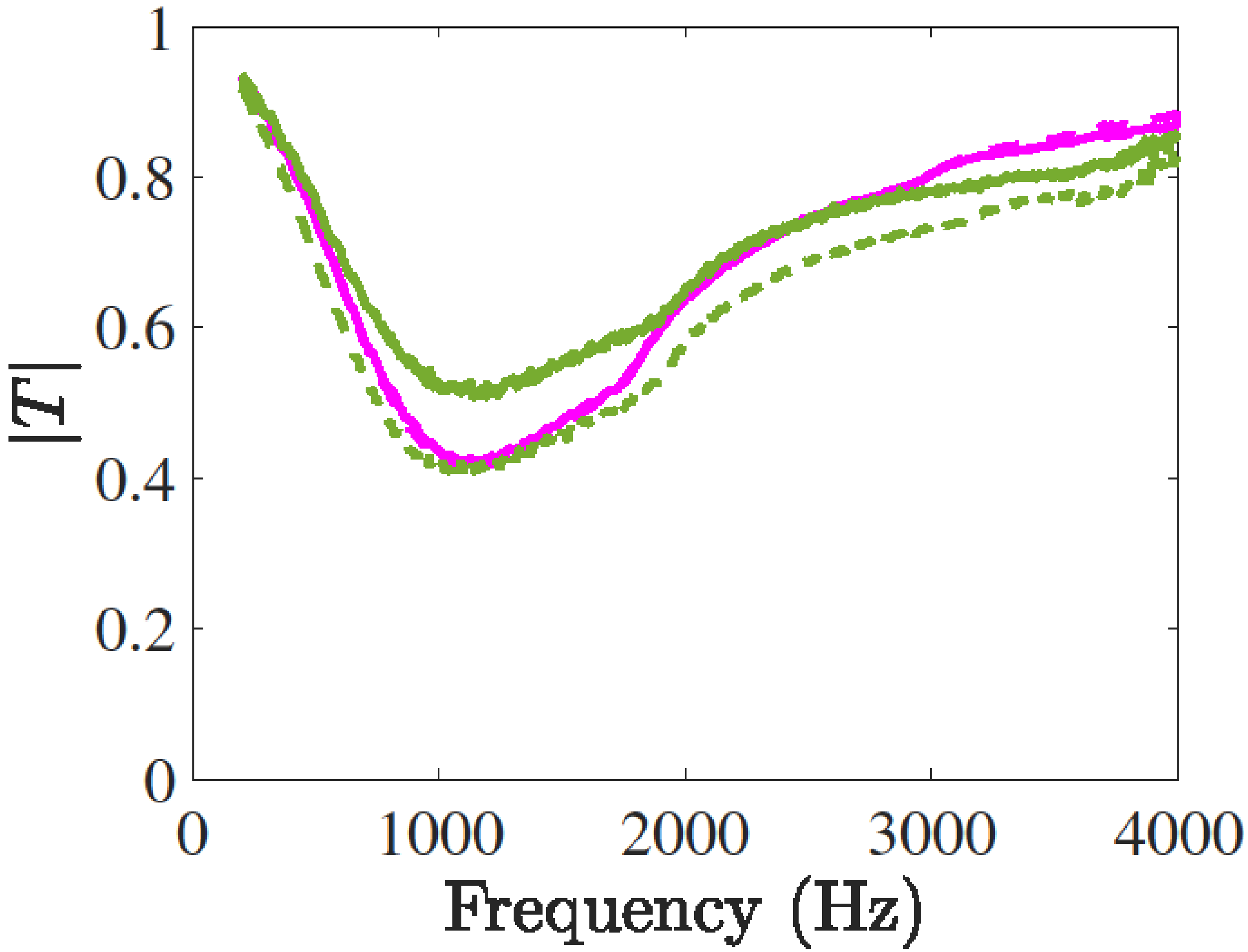

- In purple, the transmission curves for the no flow, *with* Kevlar case. Attenuation can be seen around the characteristic frequency of the resonator
- In green the same case, but for a M = 0.073 flow case. No whistling !

Comparison: with/out Kevlar

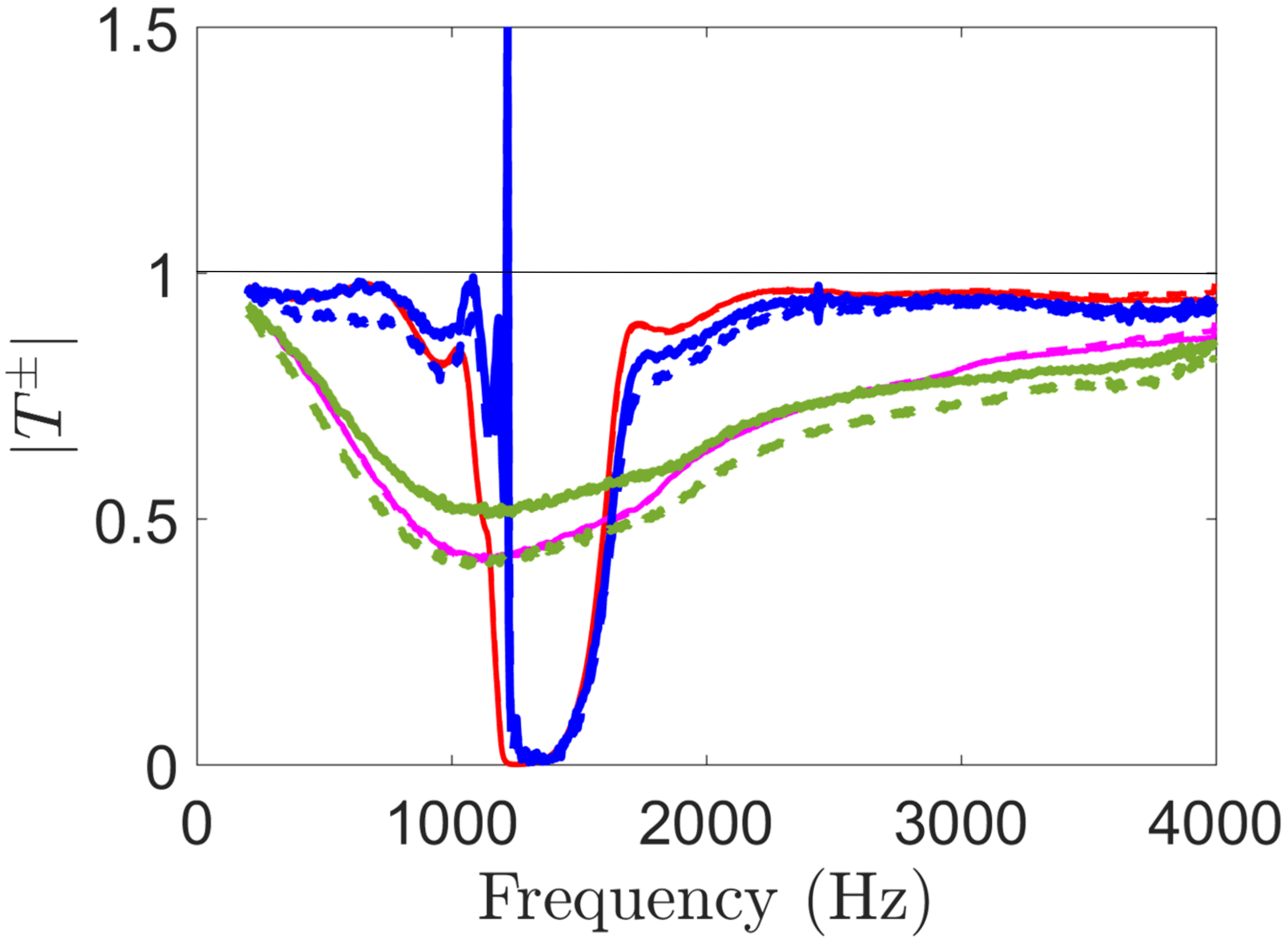

- It is appreciable the difference in behaviour: without kevlar, the effect of flow on the metamaterial is an induced whistling. With kevlar, the whistling disappears and transmission curves become flattened

Micro-slit systems

But the effect of flow could be not only overcome,
but even be taken advantage of…

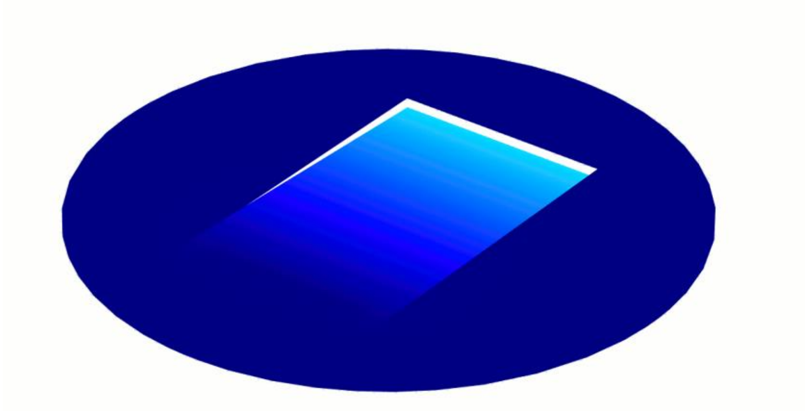

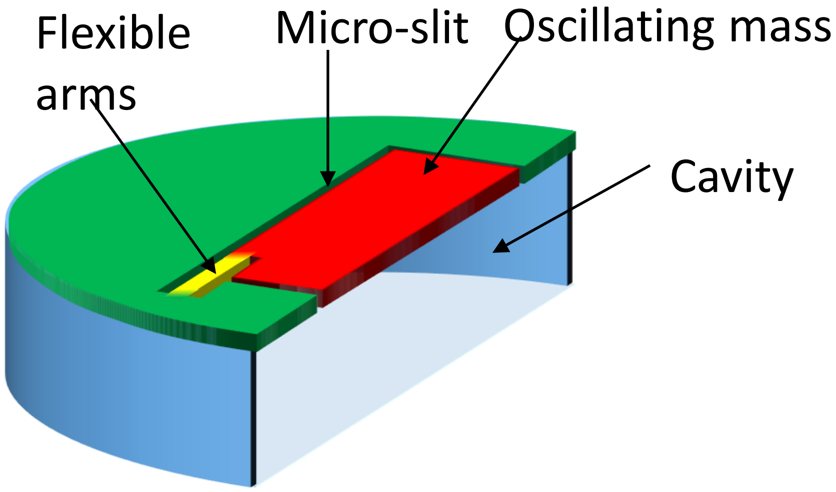

Leakage = Resistance

Micro-slit systems

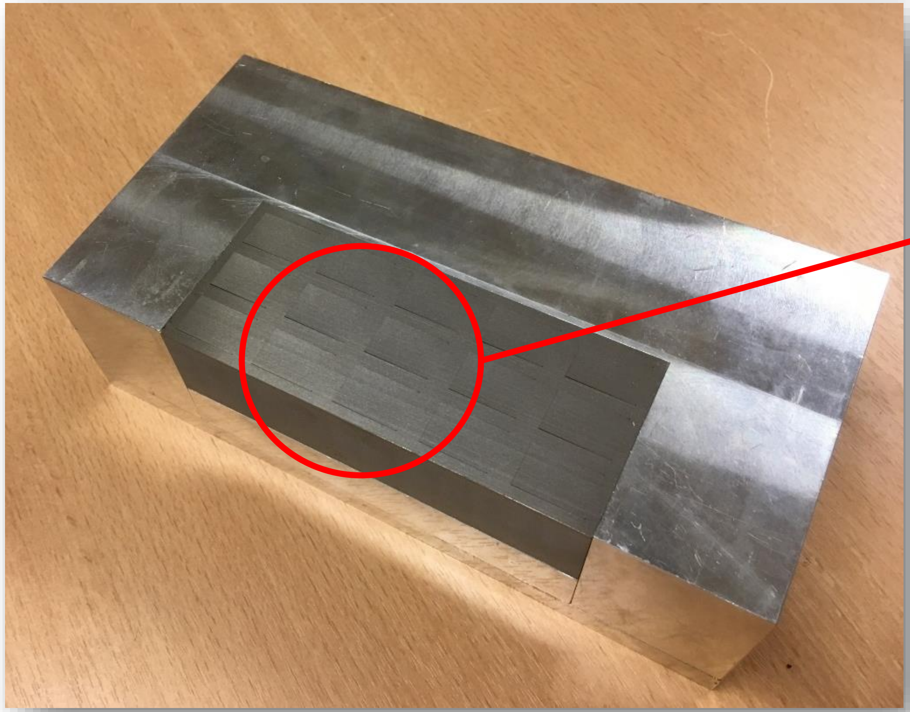

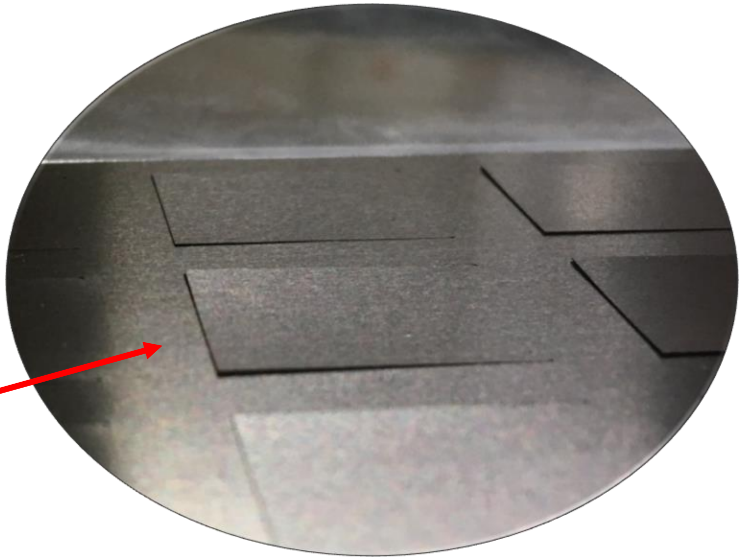

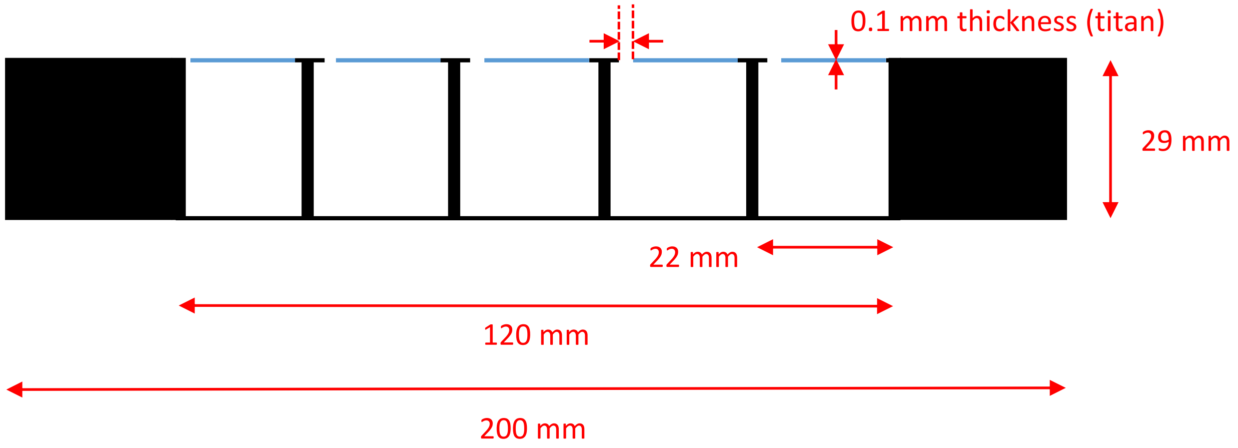

Acoustic Measurements

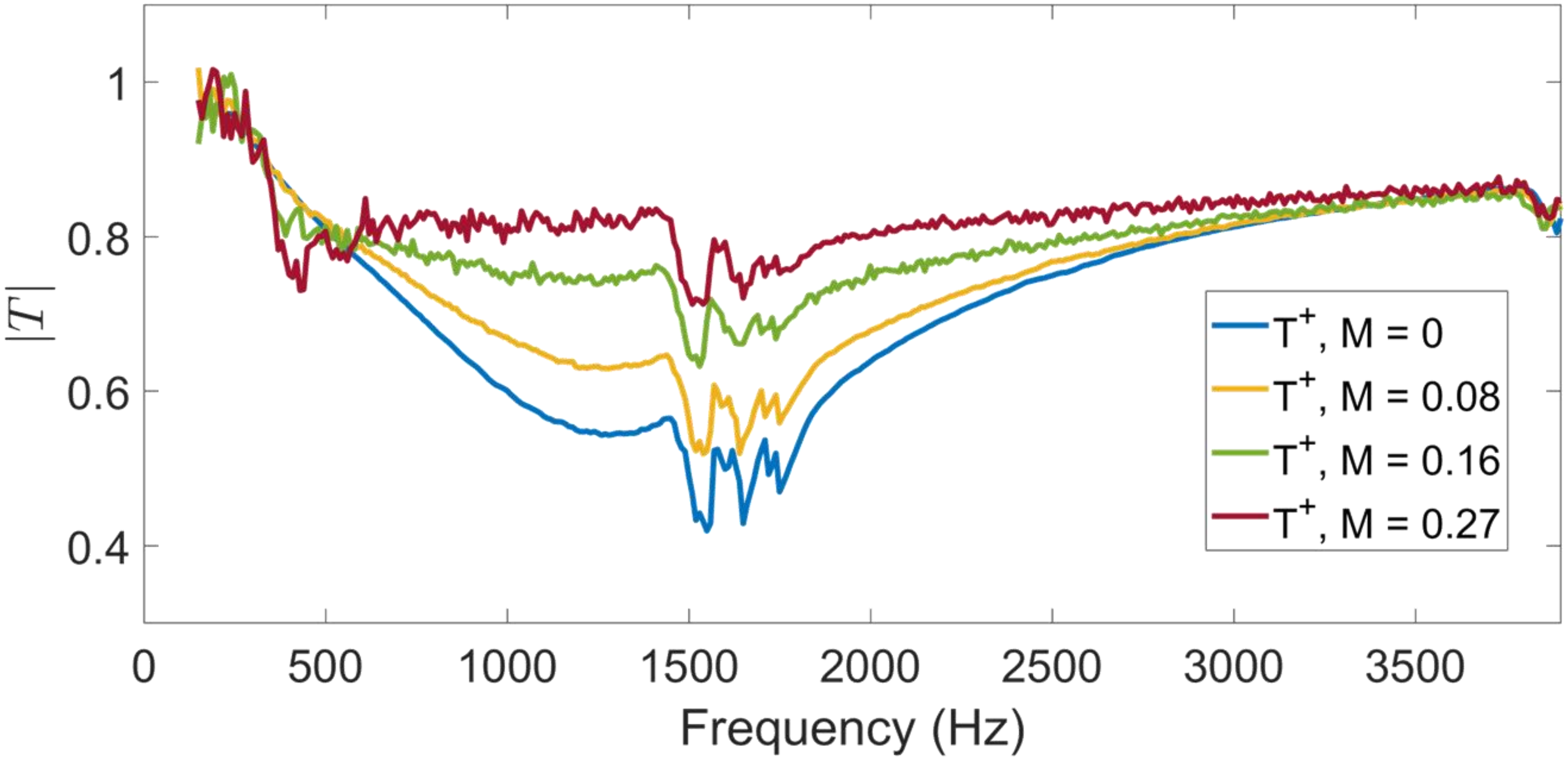

Source in Upstream position

Acoustic Measurements

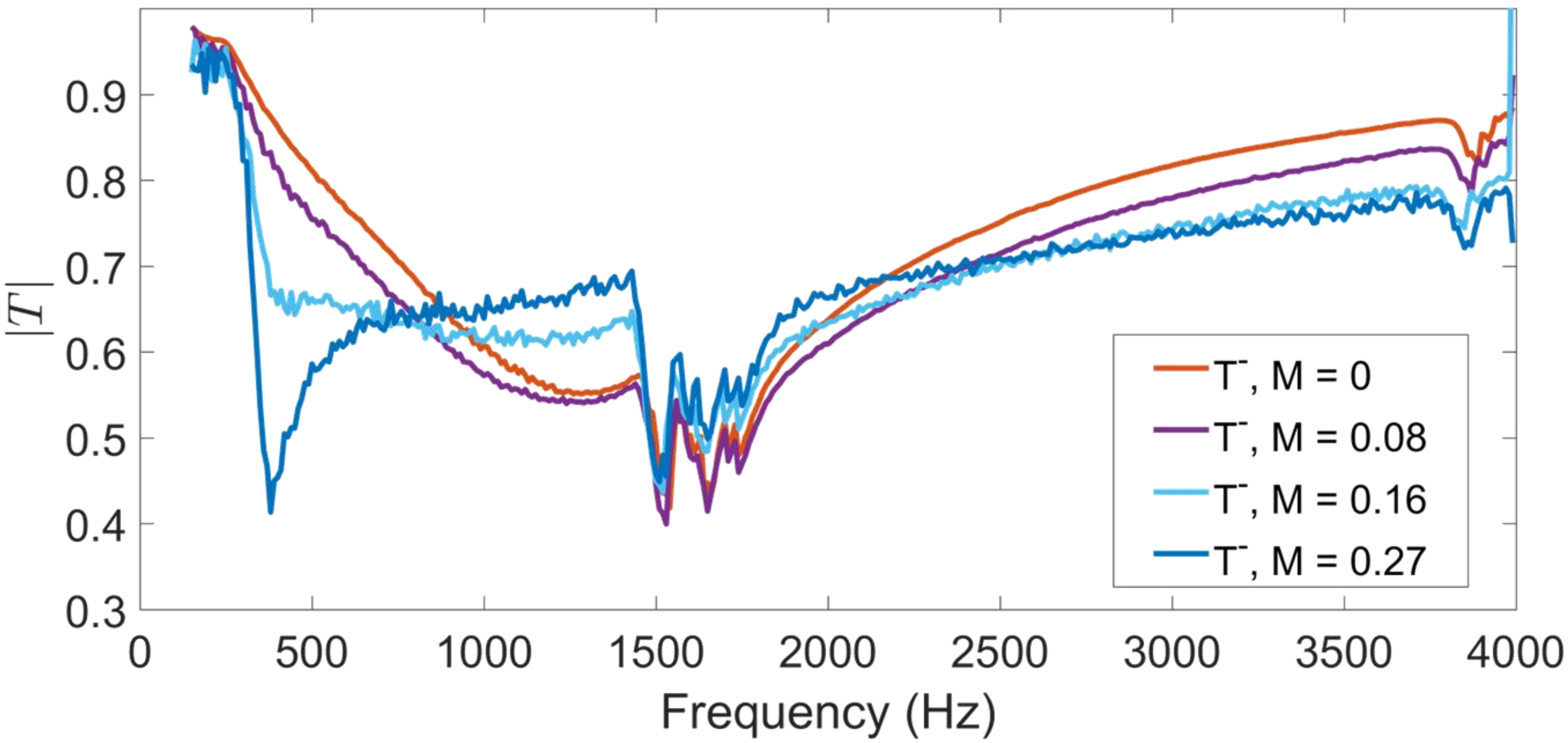

Source in Downstream position

Multi-Modal Method

First Step: Numerical investigation of 1 beam + cavity

Propagation without flow

$$k^2 P - \omega^2 P - \mathrm{d}_\mathrm{y}^2 P = 0$$

Beam

$$\begin{cases} k^4 \delta - k_M^2 \delta = -C[p]_{y=1} \\ \mathrm{i}\omega\delta = V(y=1) \end{cases}$$

Resistance

$$[p]_{y=1} = R\,V$$

Propagation in a shear flow

$$\begin{cases} \mathrm{i}(\omega - M\,k)V = -\mathrm{d}_\mathrm{y} P \\ \left(1 - M^2\right) k^2 P + 2\omega M k P - \omega^2 P - \mathrm{d}_\mathrm{y}^2 P = -2\mathrm{i}\,\mathrm{d}_\mathrm{y} M\,kV \end{cases}$$

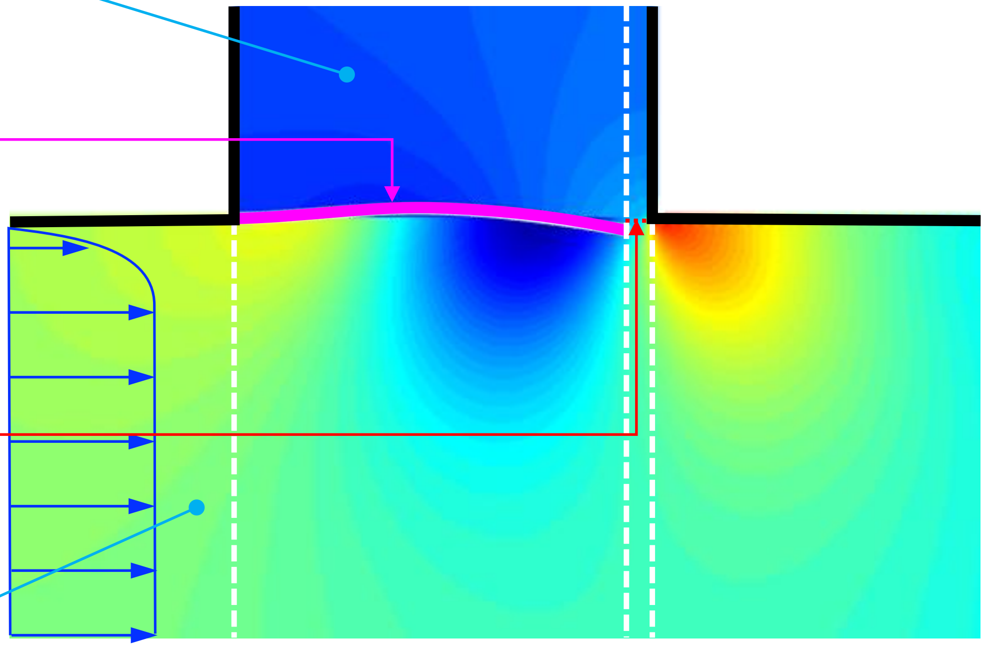

Pressure

$$p = P(y)\mathrm{e}^{\mathrm{i}(\omega t - kx)}$$

Vertical velocity

$$v = V(y)\mathrm{e}^{\mathrm{i}(\omega t - kx)}$$

Beam displacement

$$d = \delta\,\mathrm{e}^{\mathrm{i}(\omega t - kx)}$$

Multi-Modal Method

First Step: Numerical investigation of 1 beam + cavity

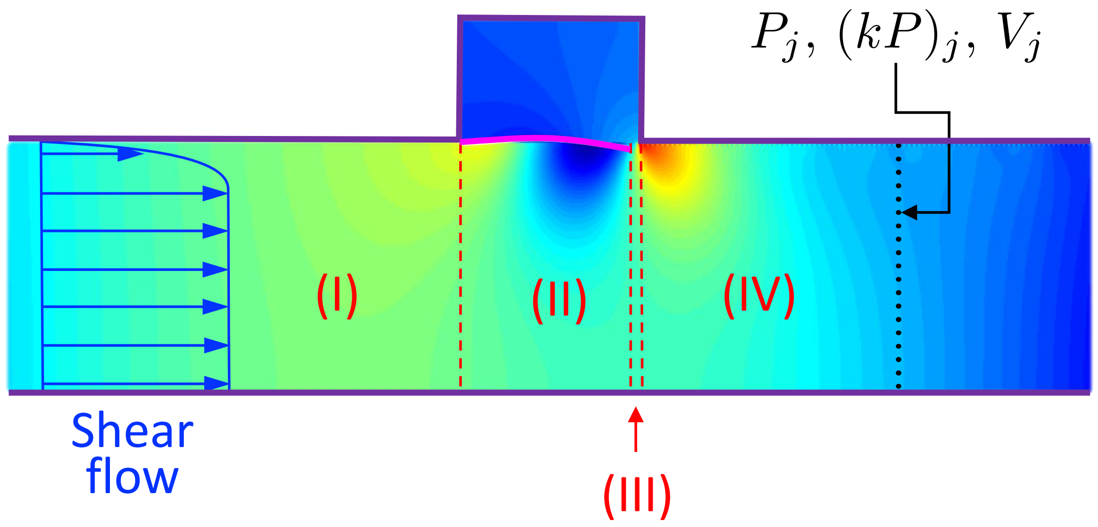

Computed by MultiModal method:

1) Discretized by Finite difference method in the transverse direction.
2) The wavenumbers and the mode shapes are computed in each zone (I, II, III and IV).
3) The unknown amplitudes of modes are computed as a function of the amplitude of the incident modes by matching the fields between the different zones.

⇒ Scattering matrix and fields

Acoustic Measurements vs MM Method

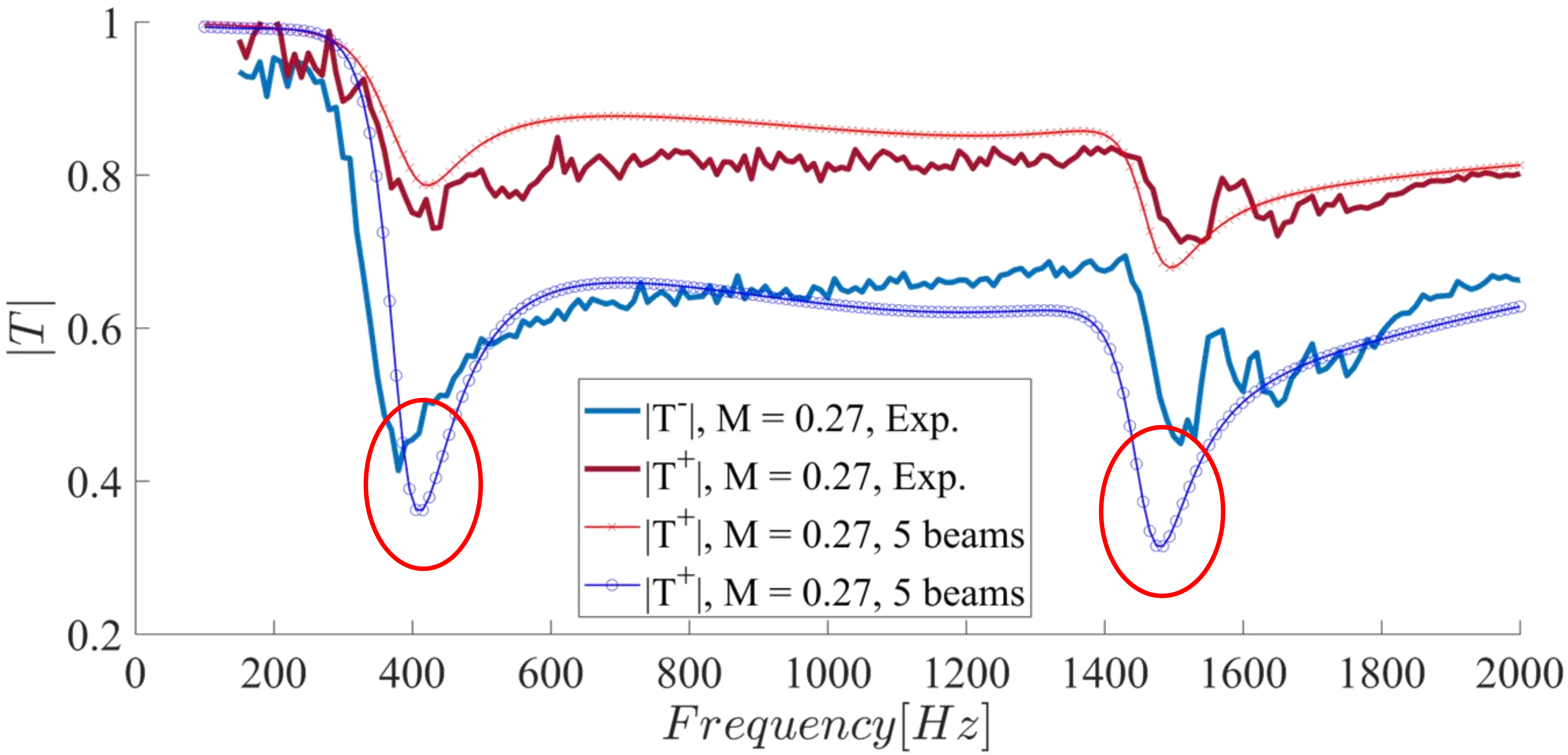

Conclusions

In contrast to the whistling case, measurements in the linear domain of corrugations show that the vorticity is distributed over the entire opening of the corrugation (and in complex formations).

We have shown that it’s still a long way for having metamaterials for with flow application, since it doesn’t exist, as of today, the needed ‘magic layer’ for the practical application

Finally, we have shown that the presence of flow could be thought as ‘useful’ when developing new passive material, so to have a positive effect rather than a detrimental one.

Smart Mitigation of flow-induced Acoustic Radiation and Transmission for reduced Aircraft, surface traNSport, Workplaces and wind enERgy noise

Electroacoustic Liners and industrial perspective

Ph.D. Student: **Emanuele De Bono**

Supervisor: **Dr. Manuel Collet**

European Union's Horizon 2020 Programme No. 722401

What are Active Liners?

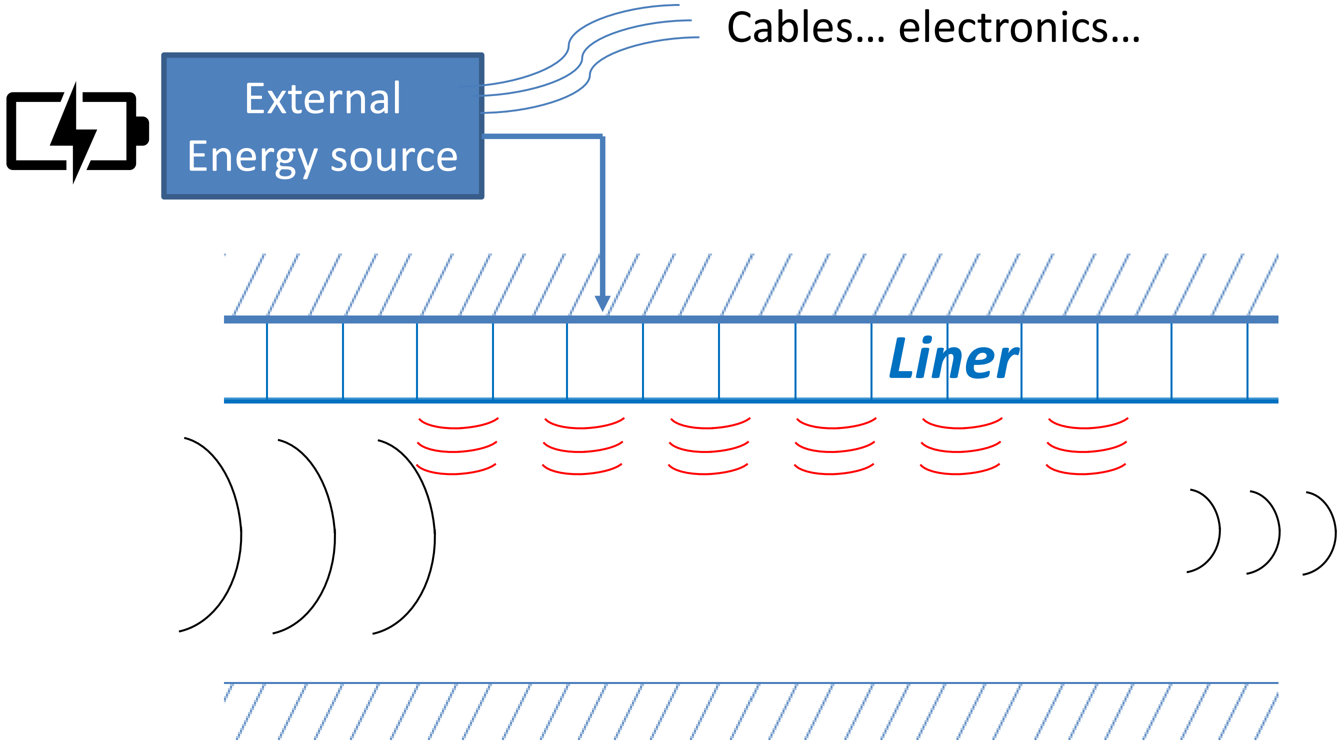

Why Active Liners?

passive liners limitations

- Different flight phases → Different frequencies to target

- UHBR… not enough space

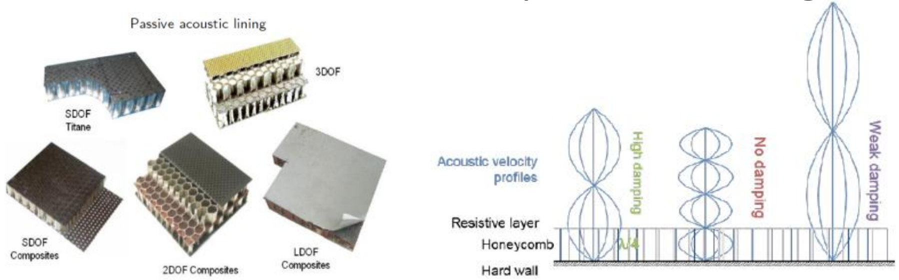

Credit: H. Lissek

- Causality and passivity conditions constrain thickness

$$d \geq \frac{c_0}{\pi}\frac{B_{eff}}{B_0}\left|\int_0^{\infty}\frac{1}{\omega^2}\ln(|R(\omega)|)\,d\omega\right|$$

M. Yang, 2017

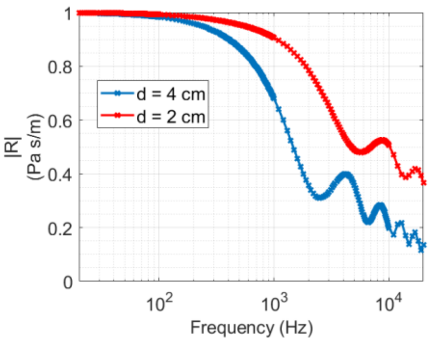

- So… can active liners do better?

Active Liners for Nacelles

- Space and thickness ✓
- Energy supply
- Robustness and stability
- Harsh environment (turbulence, heat…)

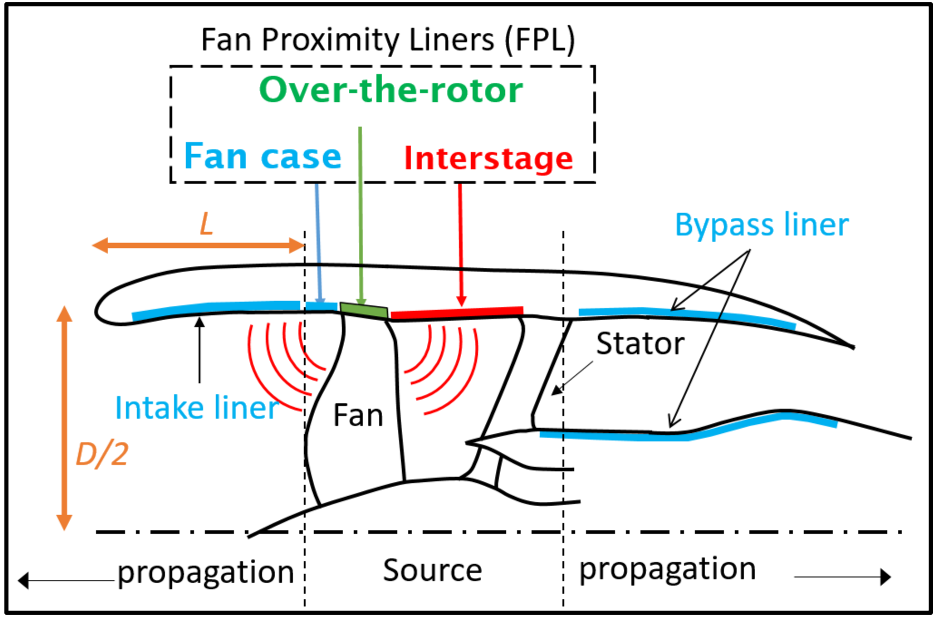

Local Impedance Control by Digitally Adaptive Loudspeaker

Pressure-based, current-driven Adaptive Loudspeaker

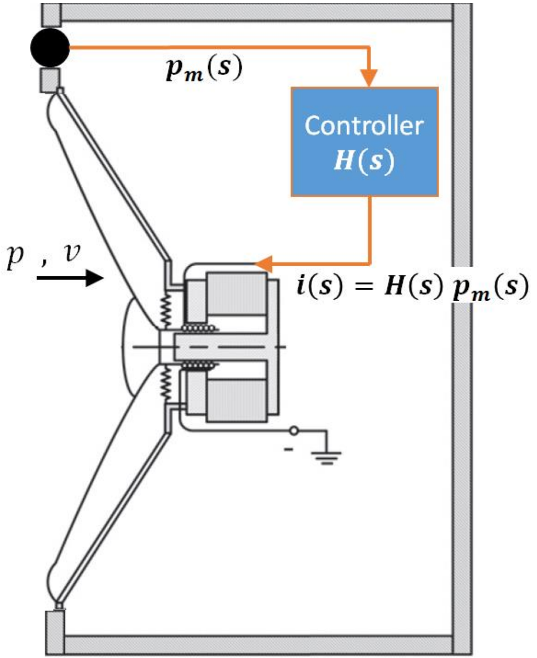

E. Rivet et al., 2016

- Mechanical dynamics model

$$Z_m^{oc}\, v(s) = S_d p(s) - Bl\, \boldsymbol{i(s)}$$

- Controller to achieve a **target local impedance $\boldsymbol{Z_{at}(s)}$**

$$i(s) = H_{loc}(s)p(s)$$

$$H_{loc}(s) = \frac{1}{Bl}\left(S_d - \frac{Z_m^{oc}(s)}{\boldsymbol{Z_{at}(s)}}\right)$$

Factors affecting the acoustical passivity

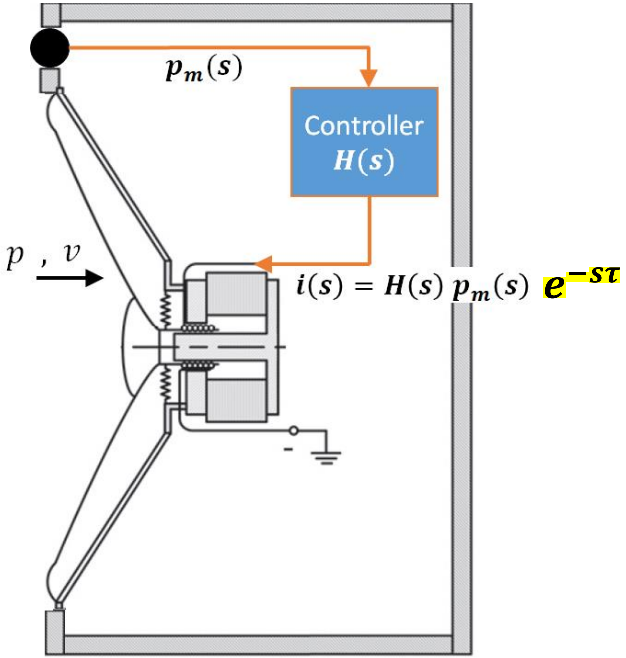

E. Rivet et al., 2016

- Time delay of the digital controller
- Mechanical dynamics model inaccuracy:
  - SDOF model uncertainties
  - Unmodelled higher order modes: *spill-over effect*
- Non-perfect collocation at high frequencies:
  The average pressure on the speaker diaphragm might not coincide with the value retrieved by the *quasi-collocated microphones.*

Digitally Adaptive Loudspeaker and Acoustical Passivity

PASSIVE RESONATOR

Passivity and causality condition constrain the minimum compliance (or thickness)

$$C_a = \frac{1}{K_a} \geq \frac{1}{\pi \rho_0 c_0} \left| \int_0^{\infty} \frac{1}{\omega^2} \ln(|R(\omega)|)\, d\omega \right|$$

M. Yang, 2017

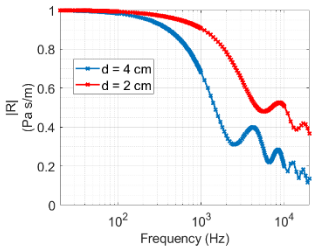

ACTIVE RESONATOR

Passivity and causality conditions constrain the minimum amplitude of static controller

$$|H_{loc}(s \to 0)| \geq \frac{S_d}{Bl} \left(\frac{K_a}{\pi \rho_0 c_0} \left| \int_0^{\infty} \frac{1}{\omega^2} \ln(|R(\omega)|)\, d\omega \right| - 1 \right)$$

E. De Bono, 2020

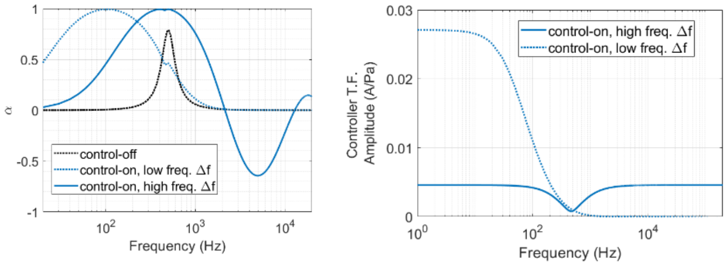

Digitally Adaptive Loudspeaker and Acoustical Passivity

Example: *passive absorber used to restore high frequency passivity*

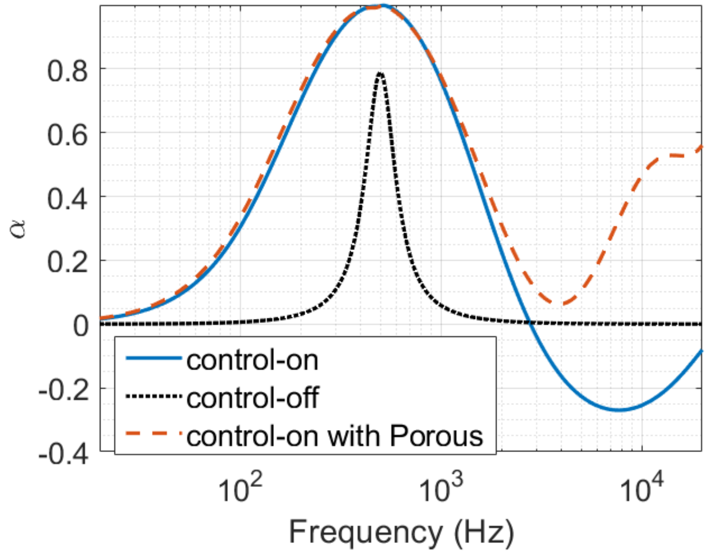

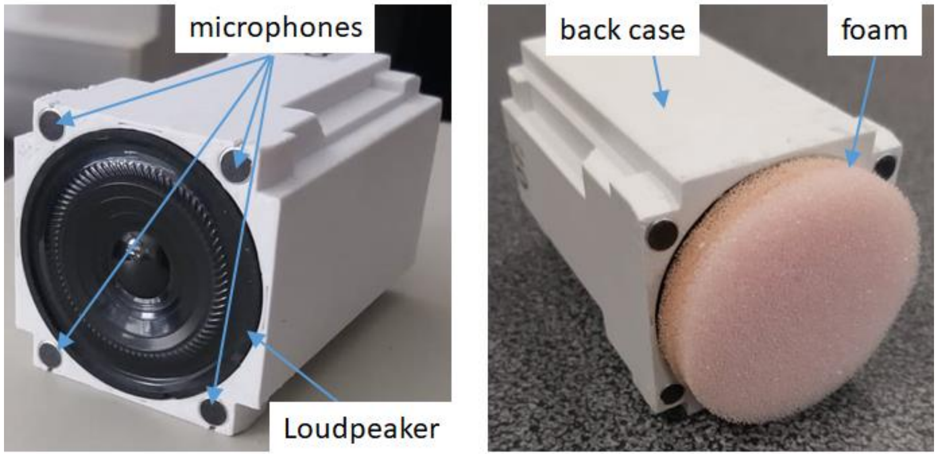

Digitally Adaptive Loudspeaker And Energy supply

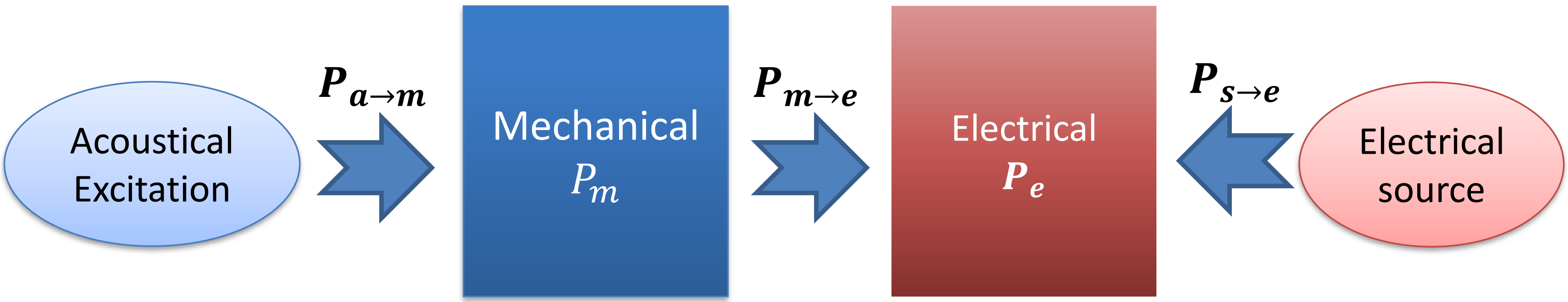

$$Z_m^{oc}\, v(j\omega) = S_d p(j\omega) - Bl\, i(j\omega)$$
$$Z_e(\omega) i(j\omega) = u(j\omega) + Bl\, v(j\omega)$$

$$P_m = P_{a\to m} - P_{m\to e}$$
$$P_e = P_{s\to e} + P_{m\to e}^*$$

Digitally Adaptive Loudspeaker And Energy supply

- The energy supply depends on how much we move away from the loudspeaker own ***reactive behaviour***

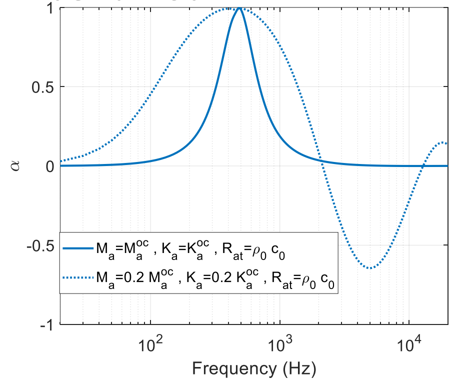

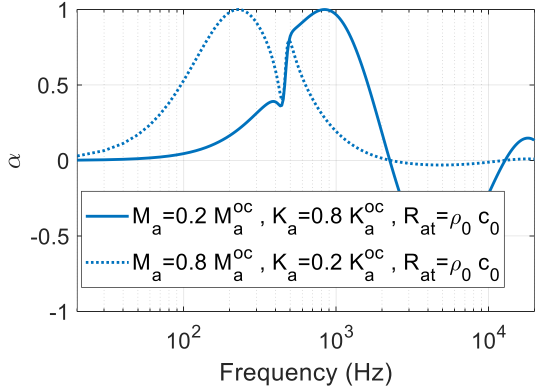

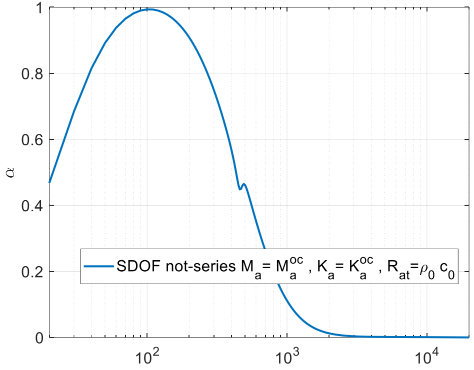

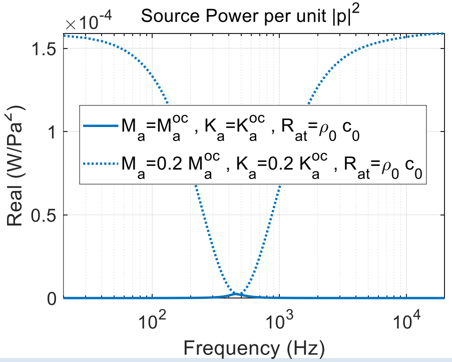

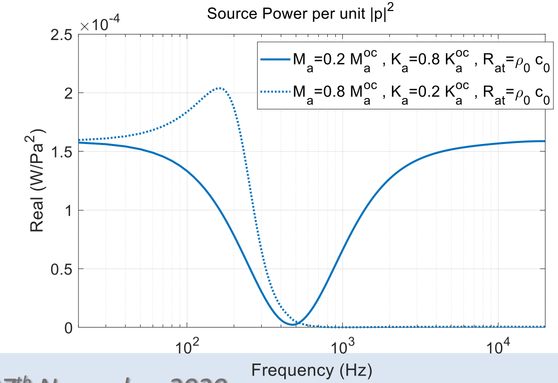

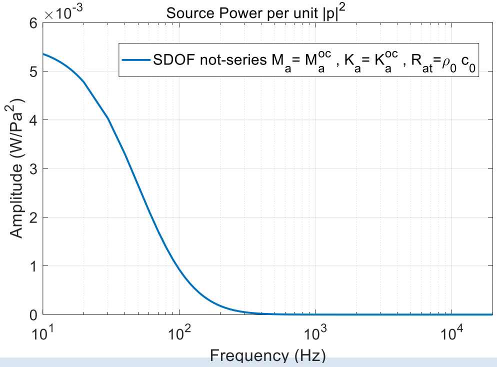

From Local to "Non-Local" boundary control

$$Z_a[\partial_t v_n(t,x)] = \partial_t p(t,x) + c_a \partial_x p = D_t\Big|_{c_a} p(t,x)$$

$$Z_m^{oc}\, v(s) = S_d p(s) - Bl\, \boldsymbol{i}(\boldsymbol{s})$$

$$\boldsymbol{i}(\boldsymbol{s}) = H_{loc}(s)\, p(s) + H_{grad}(s)\, \widehat{\partial_x} p$$

- Additional *acoustical passivity* condition: $|c_a| \leq c_0$

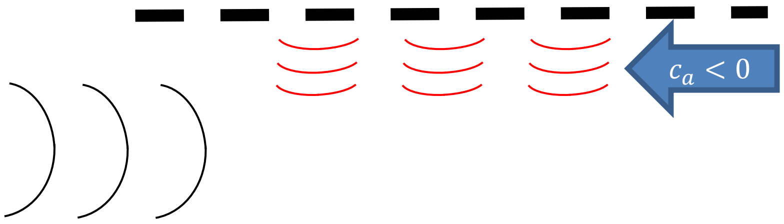

- Additional *energy supply* for $H_{grad}(s)$:

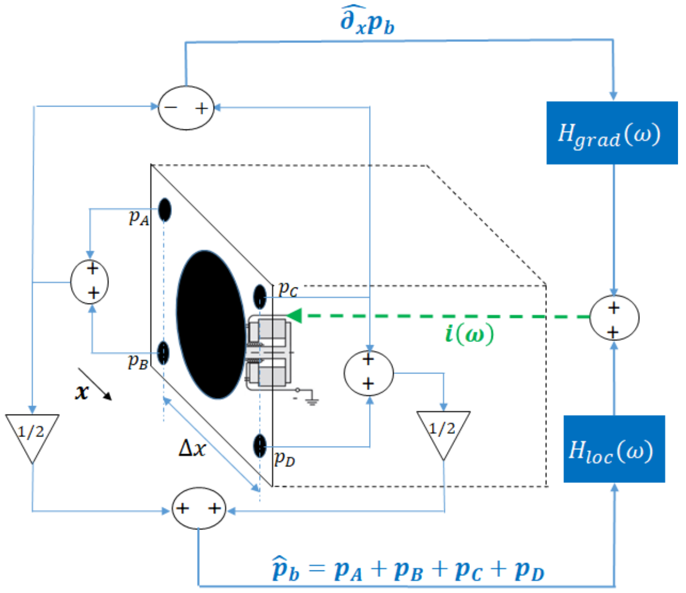

From Local to “Non-Local” boundary control

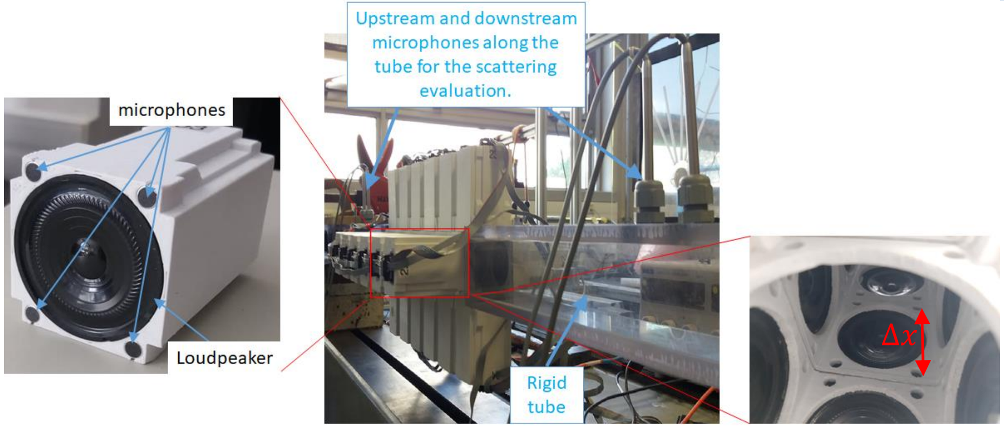

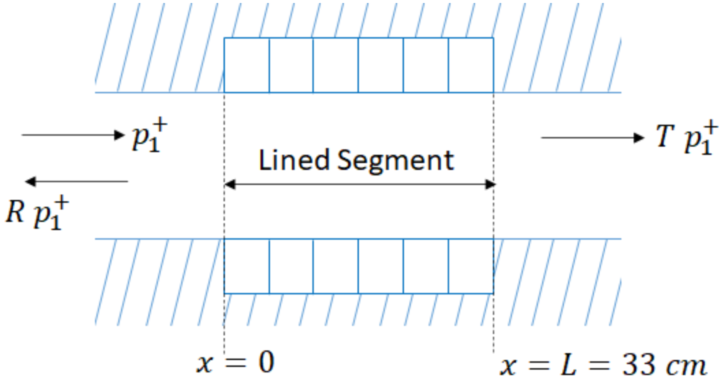

$$Z_a[\partial_t v_n] = \partial_t p + c_a \partial_x p$$

$Z_a(j\omega)$ is fixed for both “Local” and “Non-Local”

E. De Bono, 2020

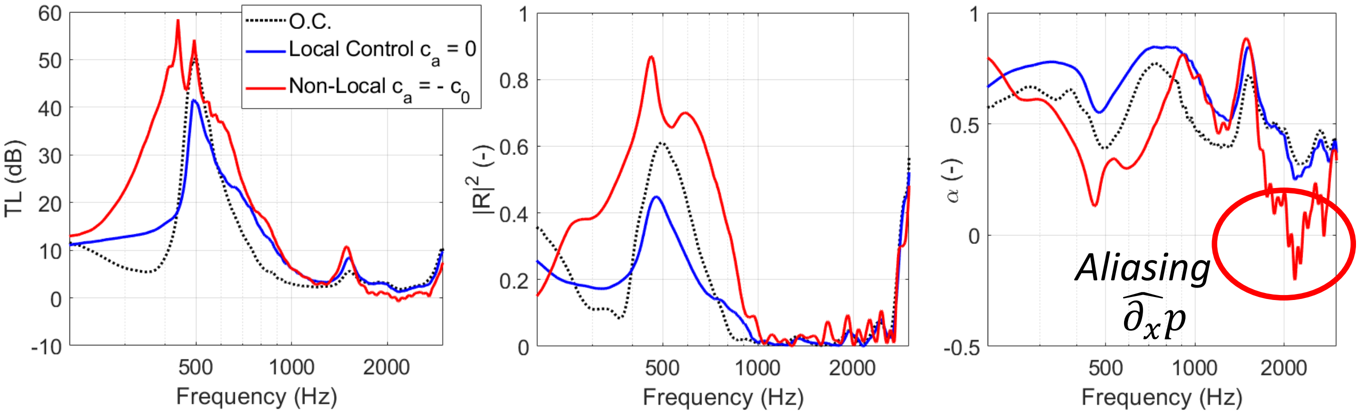

Electroacoustic liners and Flow

- Electroacoustic cells needs **protection from flow**!

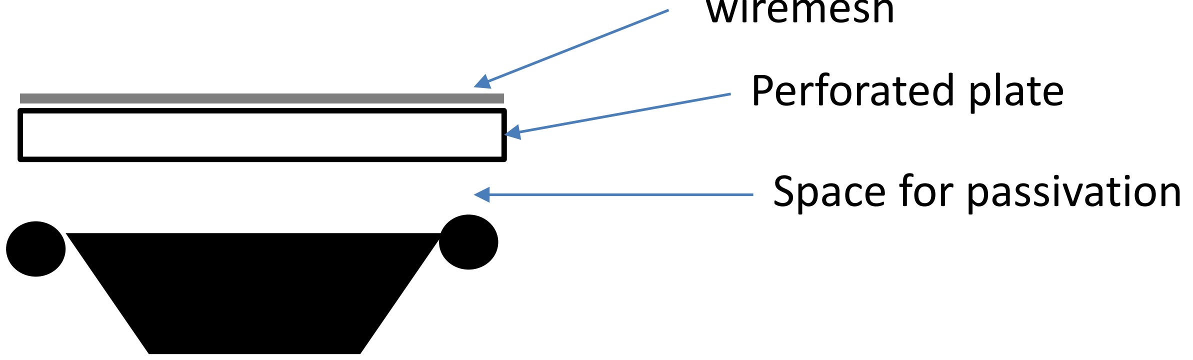

- Microphone must be chosen to resist high dB level with a sufficient sensitivity as well $$$

Next steps

- Air-flow interaction with Non-Local B.C. (convection on the boundary VS convection in the domain by Mach air-flow).

- Investigation of the Convected B.C. concept for higher-order-modes excitations.

- Optimization techniques for robustness (H_∞ , μ strategy).

- Energy harvesting potentials.

Smart Mitigation of flow-induced Acoustic Radiation and Transmission for reduced Aircraft, surface traNSport, Workplaces and wind enERgy noise

Development of Intelligent Lightweight Material Solutions for Improved Vibro-Acoustic Transmission Problems

KU LEUVEN

Early Stage Researcher (ESR) – 10

Felipe Alves Pires

SmartAnswer Public Workshop, 26th November 2020

H2020 MARIE SKŁODOWSKA-CURIE ACTIONS

Introduction

- Noise, Vibration and Harshness challenges

Ecological trend

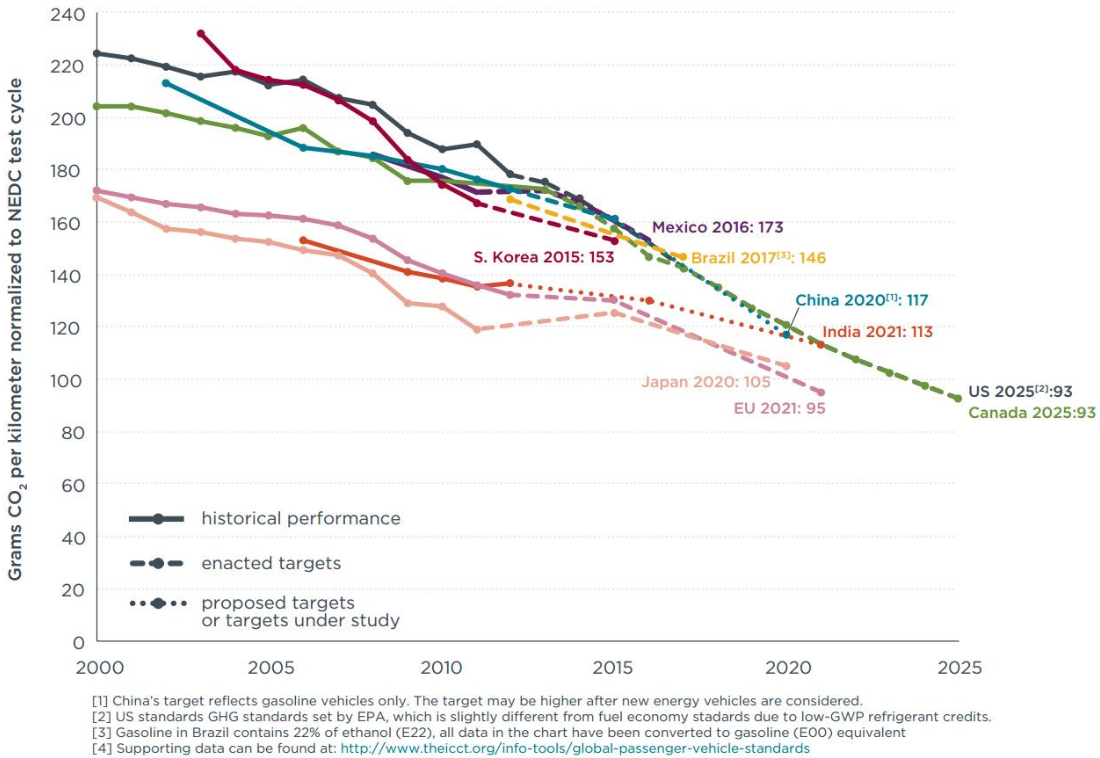

Reducing emissions

Reducing fuel consumption

Lightweight design

Worse NVH properties

Introduction

- Noise, Vibration and Harshness challenges

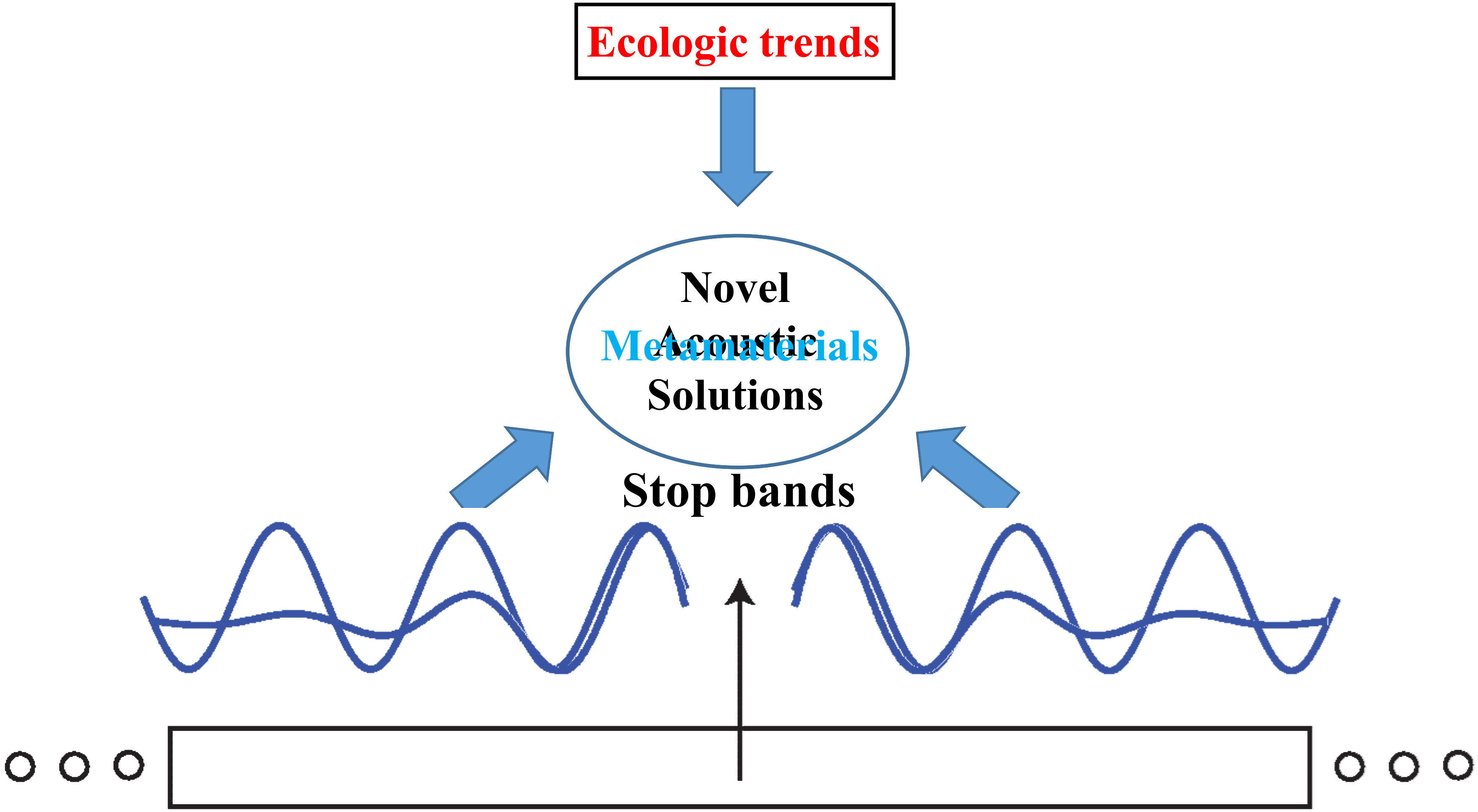

Introduction

- Resonant inclusions

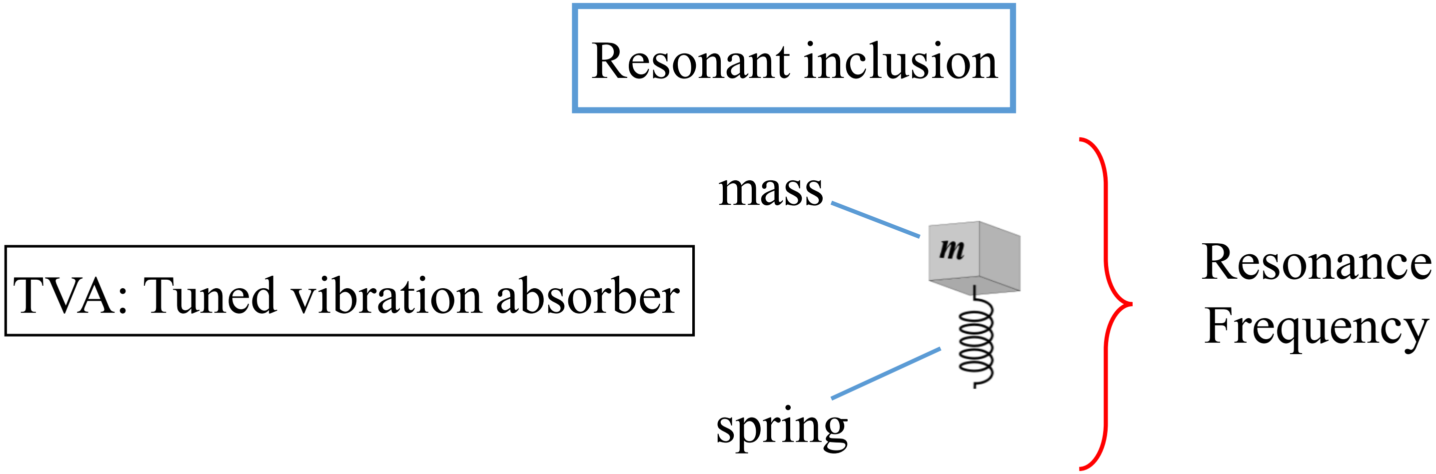

- Sub-wavelength scale: Stop band creation

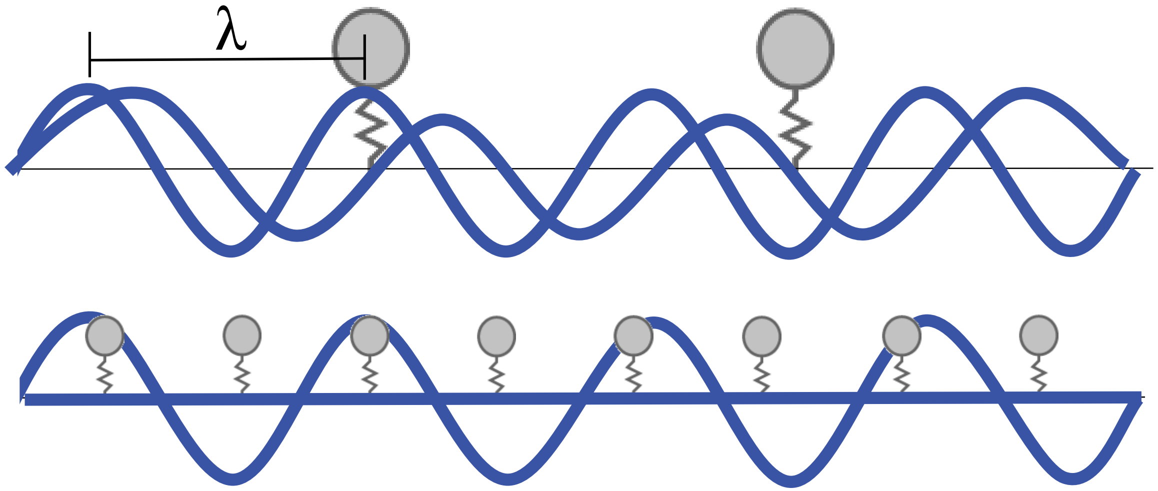

Liu, Z., et al. "Locally resonant sonic materials." science 289.5485 (2000).

Problem

PSD velocity spectrum

Flow-induced Noise and Vibrations

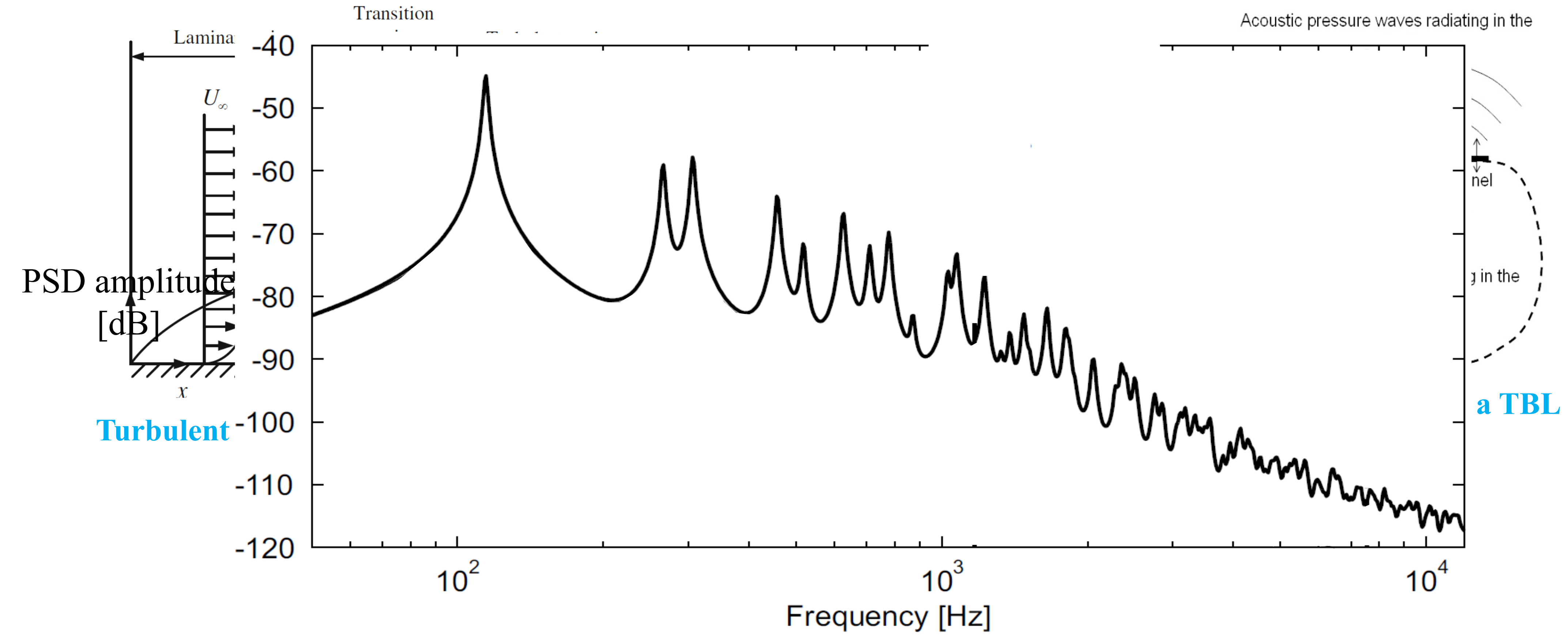

Dewan, Anupam. Tackling turbulent flows in engineering. Springer Science & Business Media, 2010.
Camussi, Roberto, ed. Noise sources in turbulent shear flows: fundamentals and applications. Vol. 545. Springer Science & Business Media, 2013.

Problem

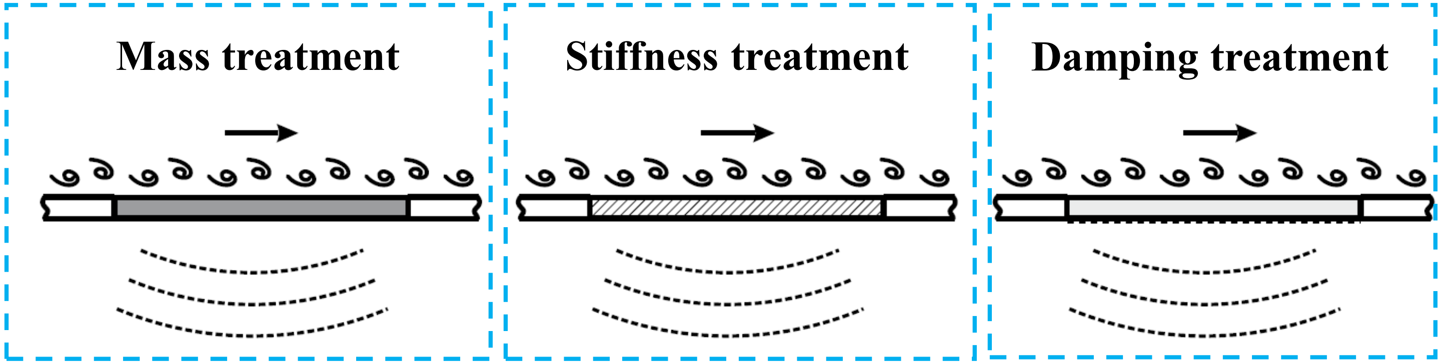

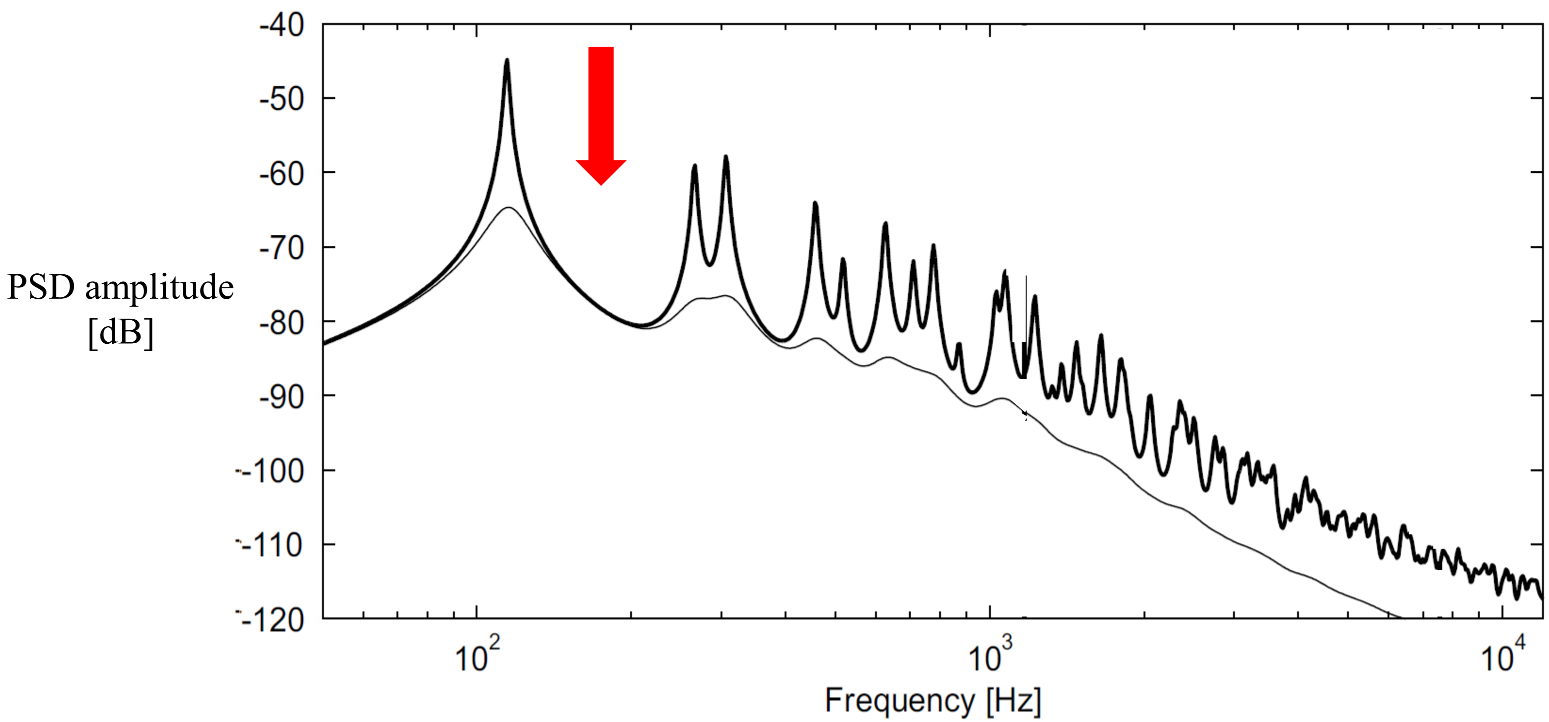

Camussi, Roberto, ed. Noise sources in turbulent shear flows: fundamentals and applications. Vol. 545. Springer Science & Business Media, 2013.

Objectives

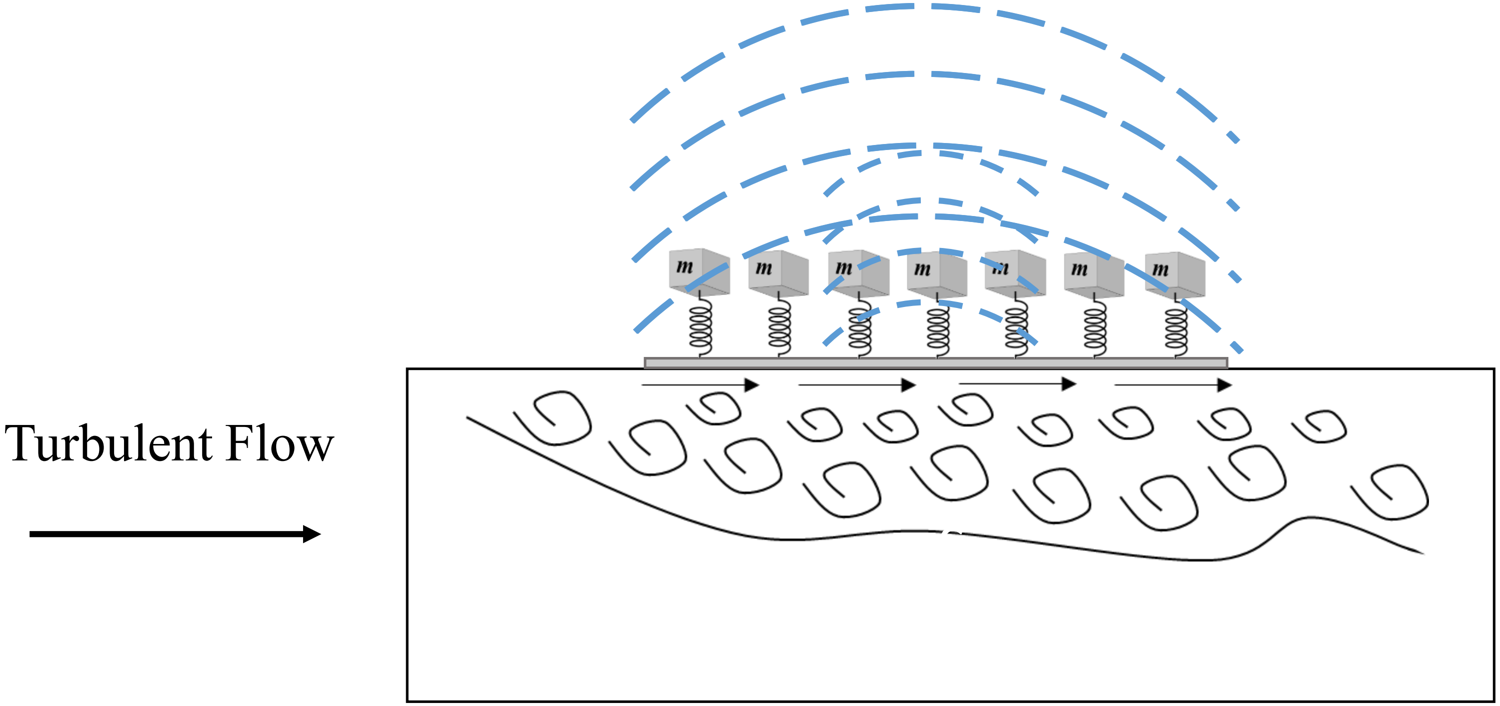

Investigate the potential of metamaterials to reduce flow-induced noise vibrations

Methodology

Flow characteristics:

- Q_{flow} = 770 m³/h
- U_{flow} = 19 m/s
- A_{duct} = 150 x 75 mm²
- Mach = 0.05

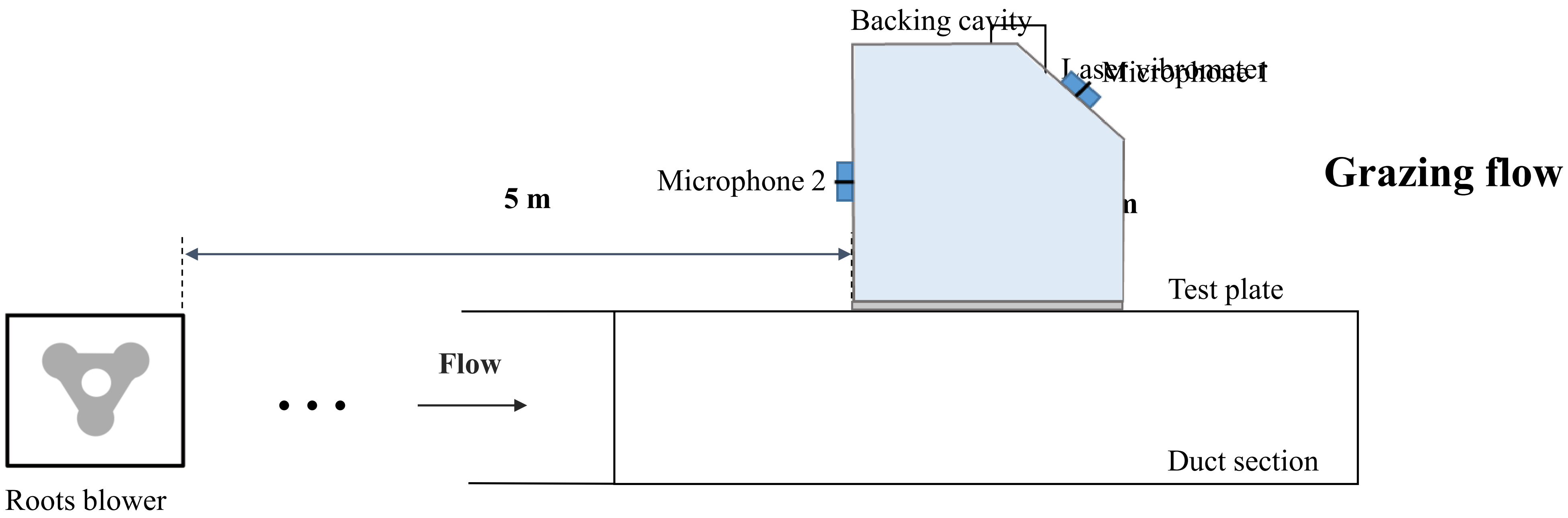

Pires, F. A., et al. "Suppression of flow-induced noise and vibrations by locally resonant metamaterials." AIAA AVIATION 2020 FORUM. 2020.

Alves Pires, Felipe, et al.; Reduction of vortex-induced vibrations by locally resonant metamaterials. Proceedings of ISMA 2020; 2020.

Experimental results - Grazing flow

BC: Clamped along its boundaries

Dimensions

- 150 x 200 x 0.5 mm

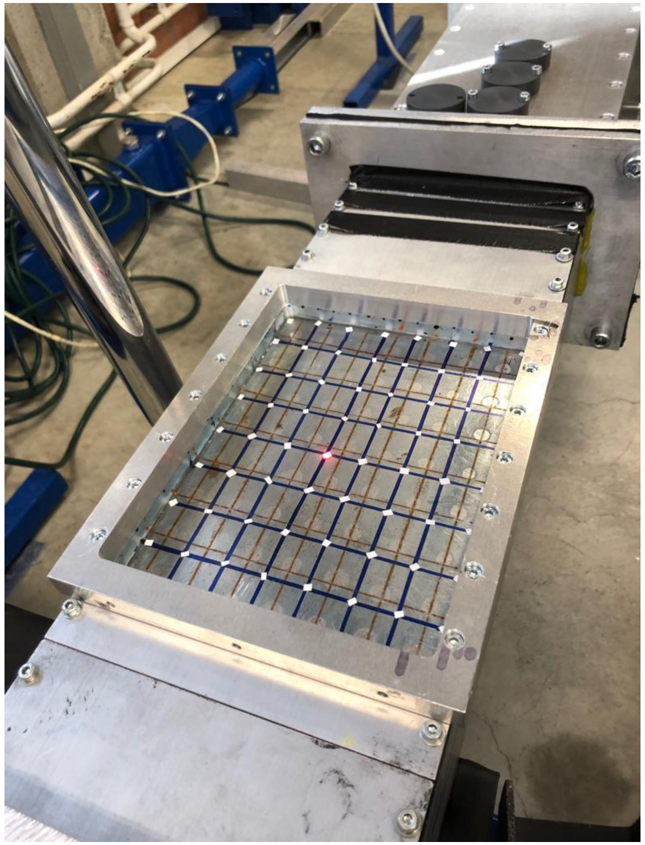

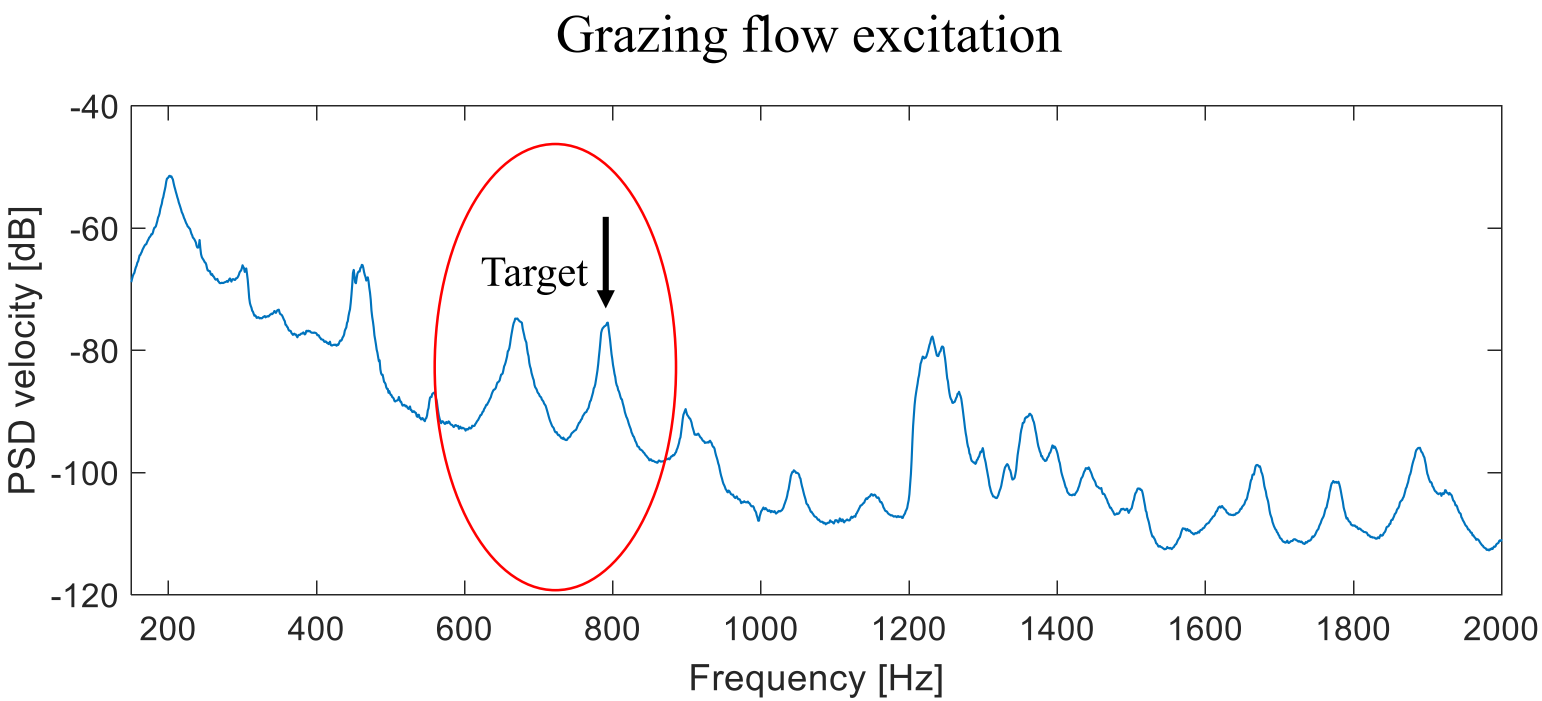

Experimental results - Grazing flow

RMS PSD pressure of the 2 microphones

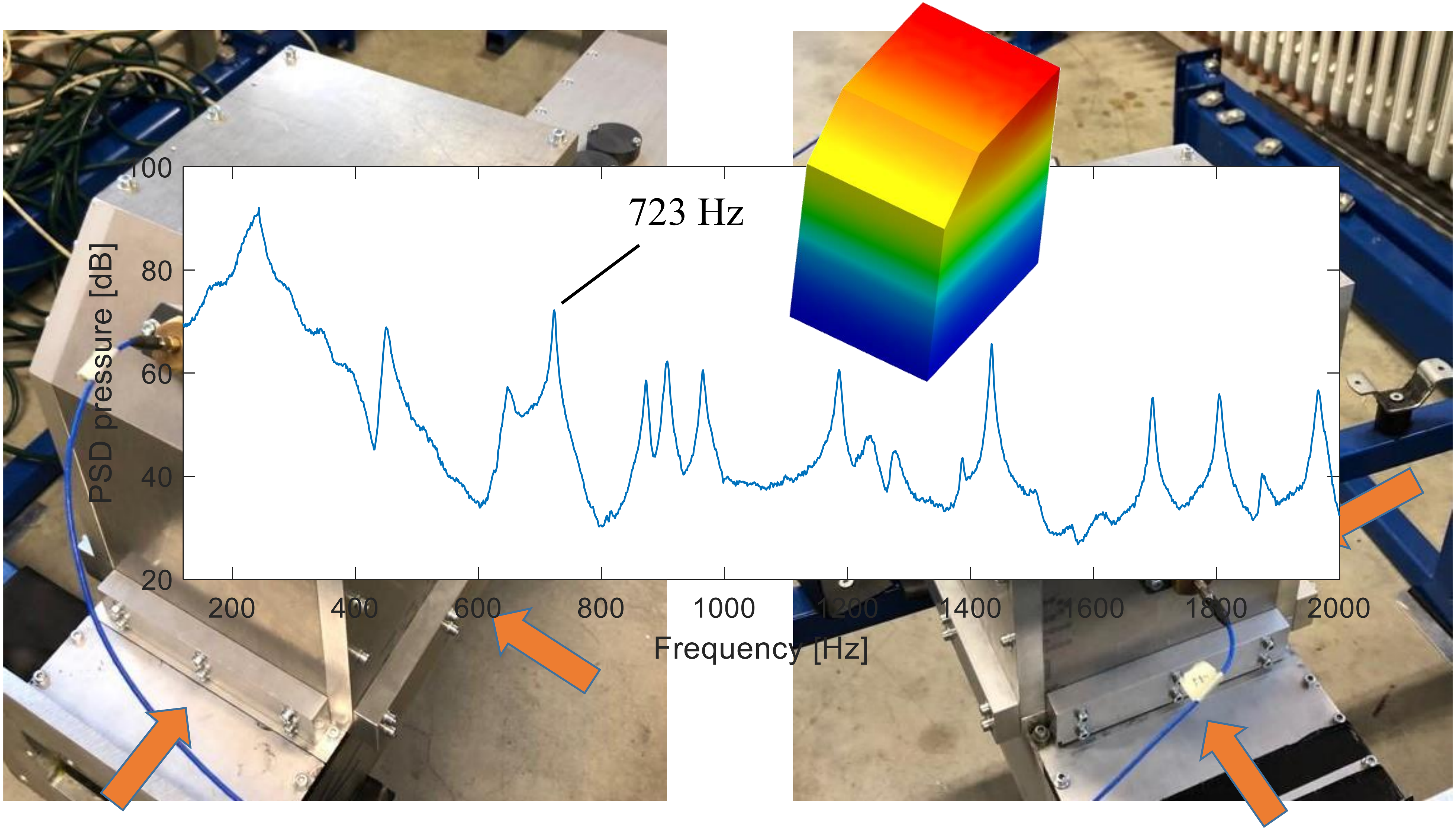

Experimental results - Grazing flow

- Mass addition: 27%

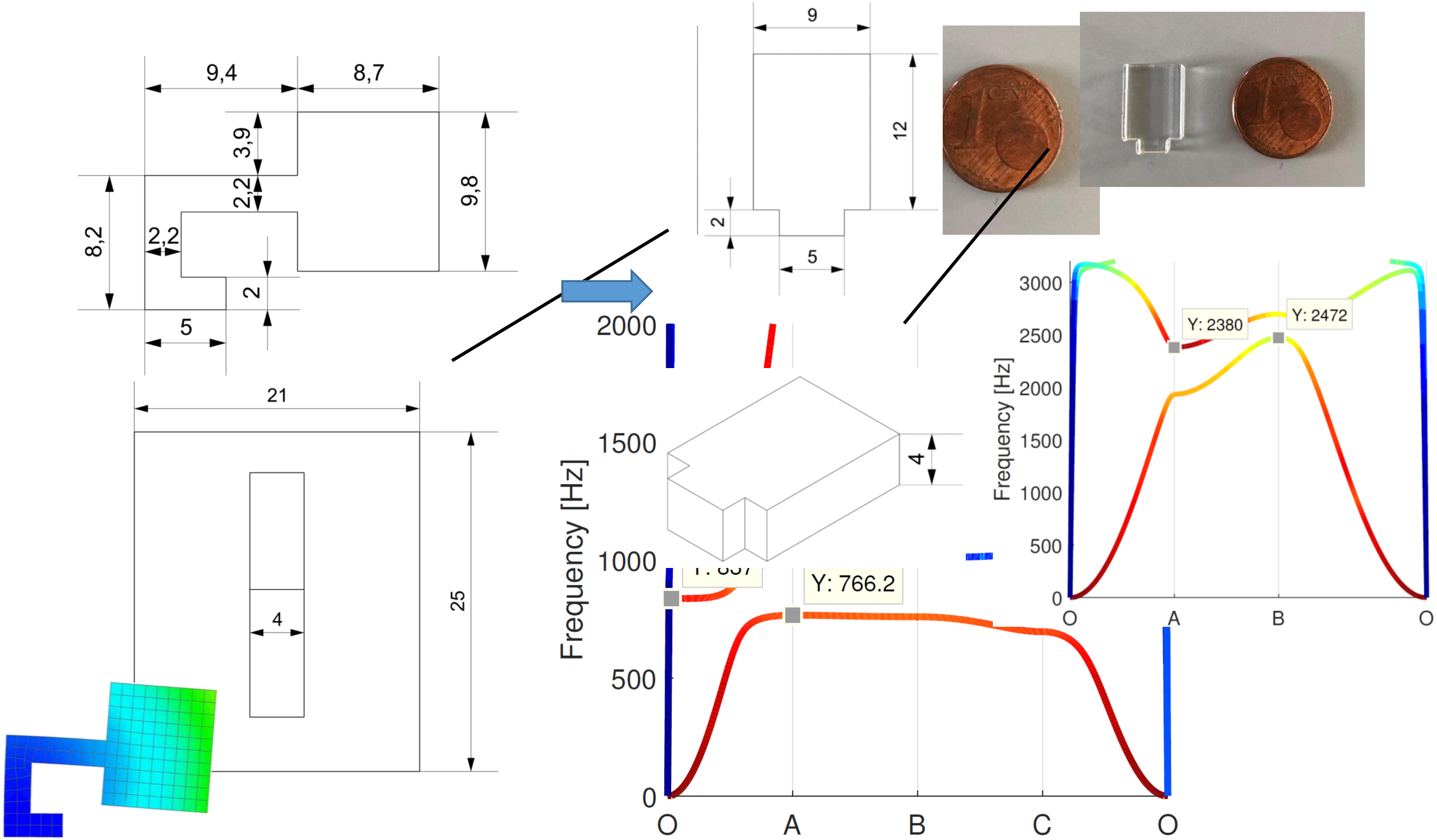

Experimental results – Grazing flow

Metamaterial configuration

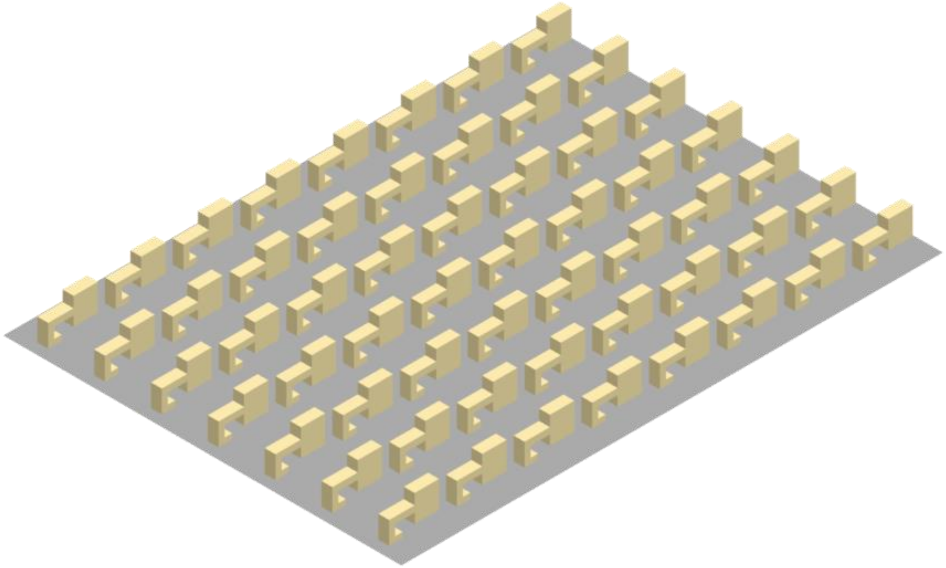

Equivalent mass

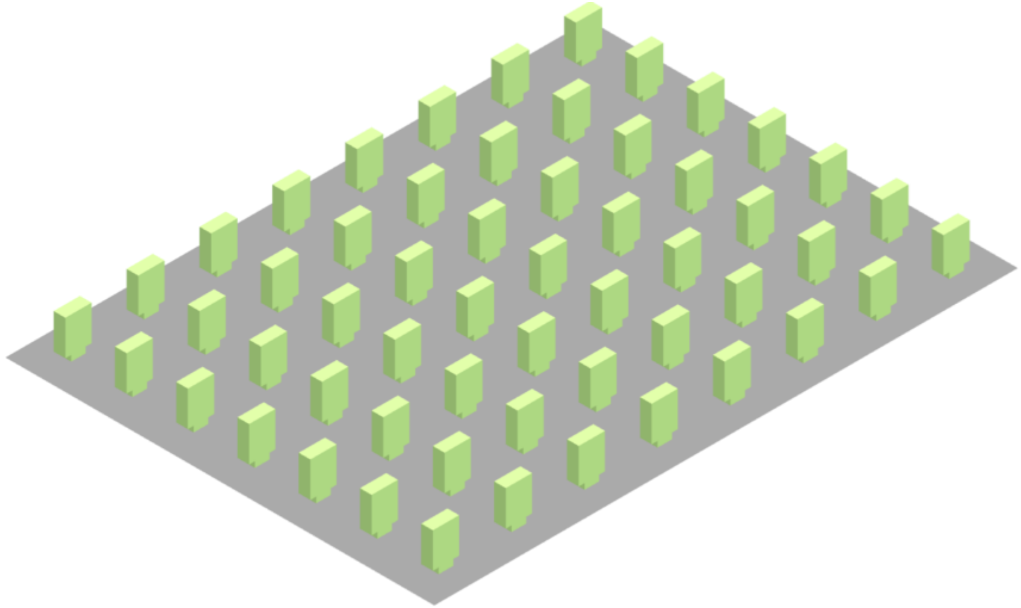

Experimental results – Grazing flow

Experimental PSD velocity response of the flat plate with and without metamaterials for U_∞ = 19 m/s for a grazing flow excitation

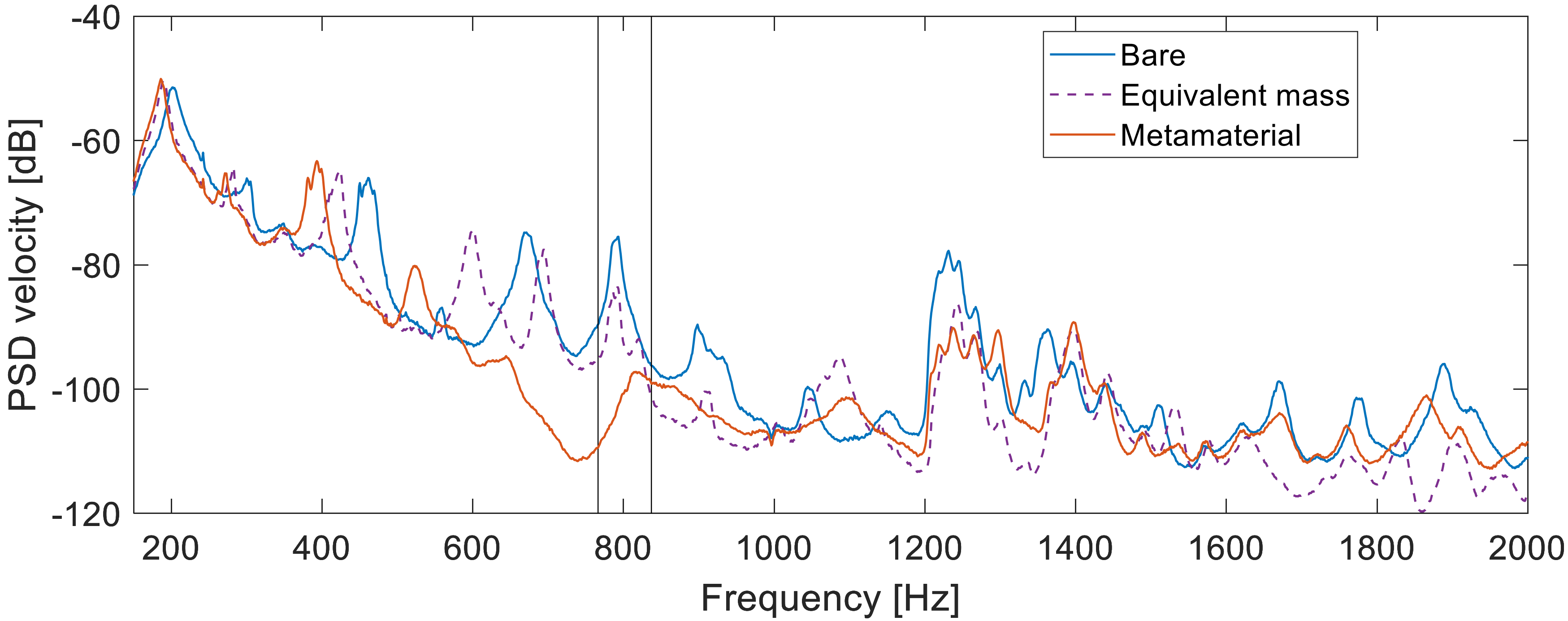

Experimental results – Grazing flow

Experimental PSD pressure response of the cavity-backed plate with and without metamaterials for $U_{\infty} = 19$ m/s for a grazing flow excitation

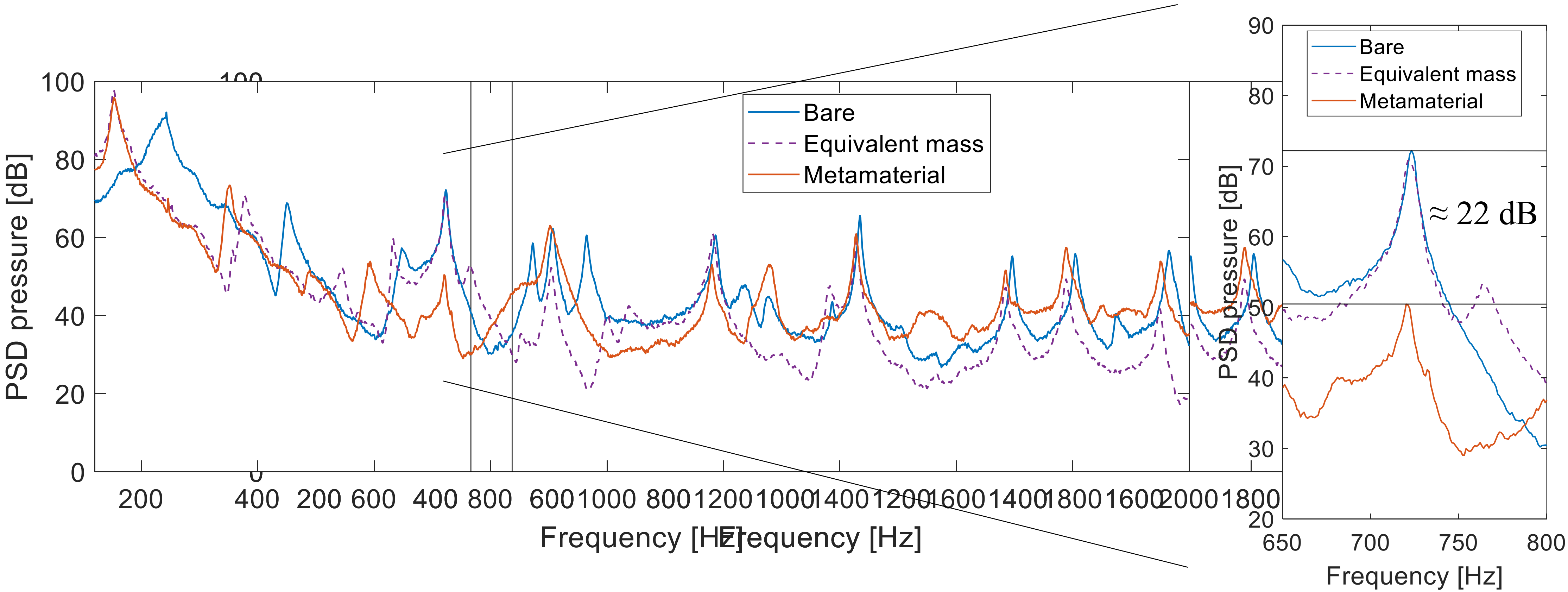

Concluding remarks

- Novel NVH solution;
- Resonance based stop bands;
- Potential to reduce flow-induced noise and vibrations:
  - ✓ Noise radiation reduction into a cavity-backed plate:
    - Grazing flow: ≈ 22 dB on a vibro-acoustic mode

Smart Mitigation of flow-induced Acoustic Radiation and Transmission for reduced Aircraft, surface traNSport, Workplaces and wind enERgy noise

SmartANSWER

Determination of Non-linear scattering matrices for perforated plates using tonal, multi and random excitation

Niloofar Sayyad Khodashenas(ESR3), Hans Bodén and Susann Boij

ROYAL INSTITUTE OF TECHNOLOGY

SmartAnswer Closure Meeting (M48) Lecture Series/Wrokshop/Consoritum meeting
VKI, Belgium, November 23rd-27th, 2020
Online Event

H2020 MARIE SKŁODOWSKA-CURIE ACTIONS

Introduction

Perforated plate

- Sound absorbers
- Small perforations
- Low porosity (percentage open area)

Main Application

- Automotive mufflers
- Aircraft engines liner
- Combustion chambers

Noise control properties influenced by

- Mean flow field
- Temperature
- Acoustic excitation level

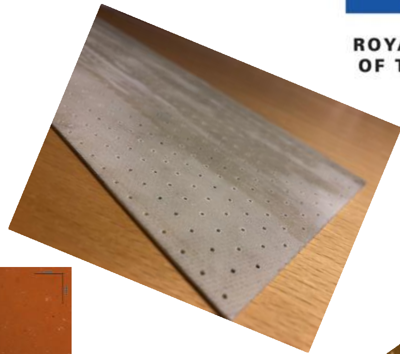

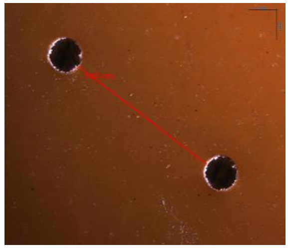

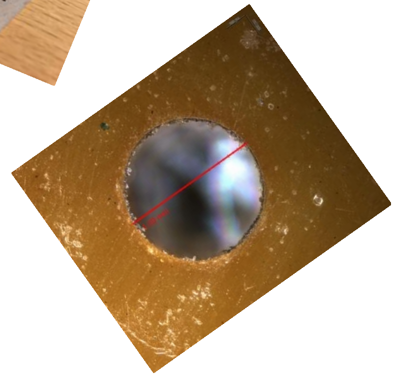

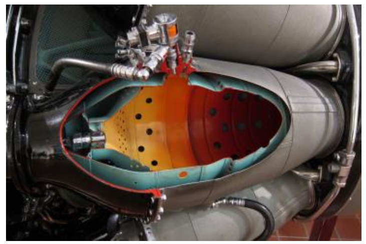

Non-Linear Mechanism

Perforated plate

↓

High particle velocity

↓

NL Phenomena

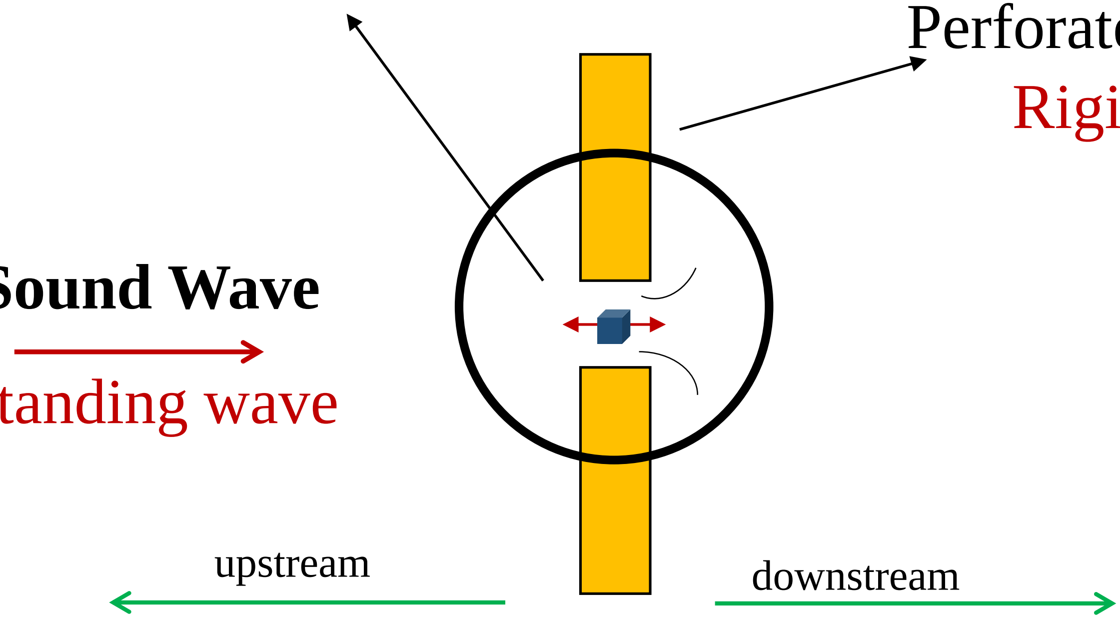

Goal { **Extract the NL properties and harmonic interactions from experiments**

Measured frequency spectrum – High excitation level

ROYAL INSTITUTE OF TECHNOLOGY

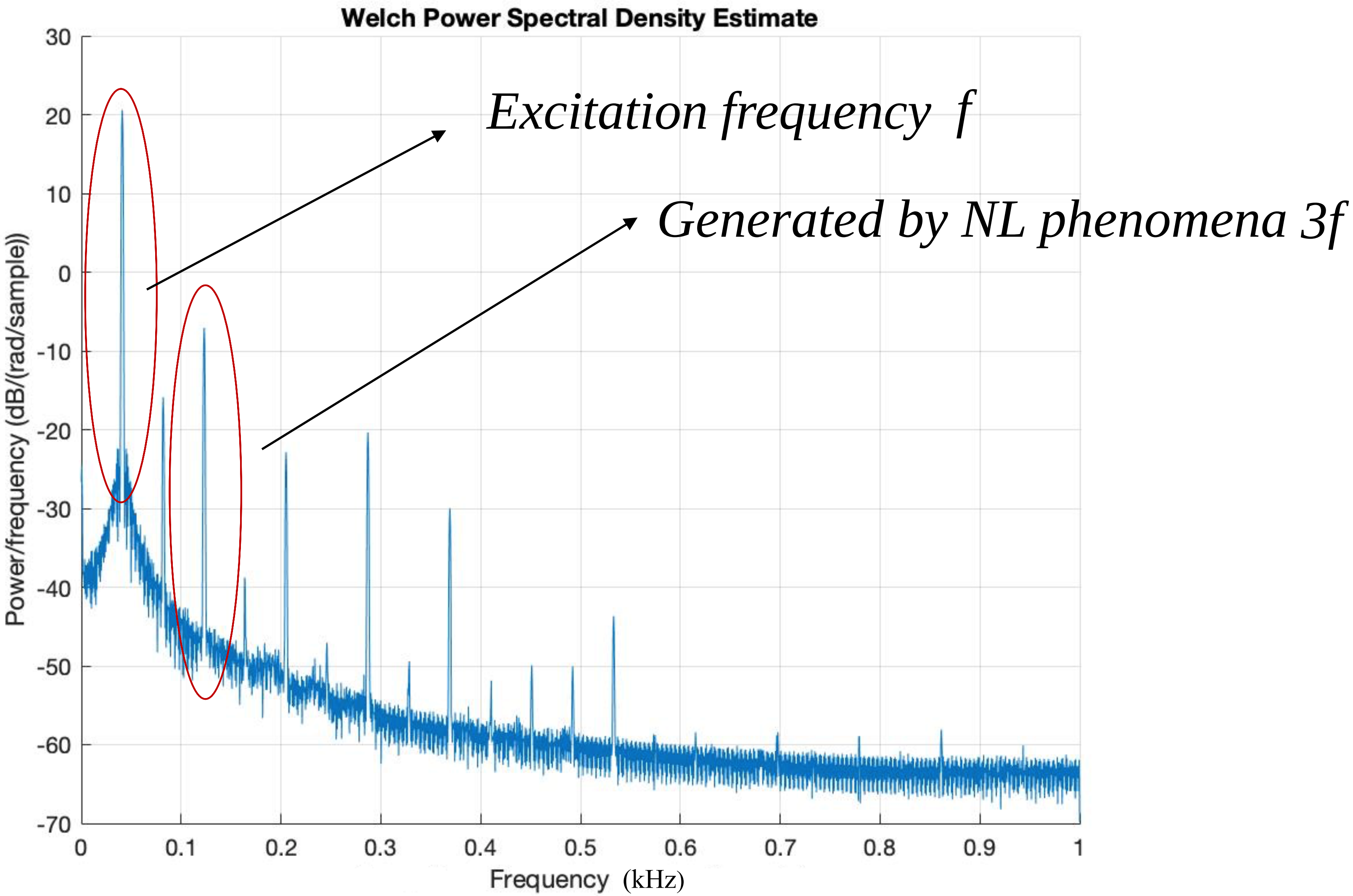

Setup at MWL Lab

Experiment Setup In MWL Lab

Schematic of experiment setup and Model

❖ Schematic of experiment Setup

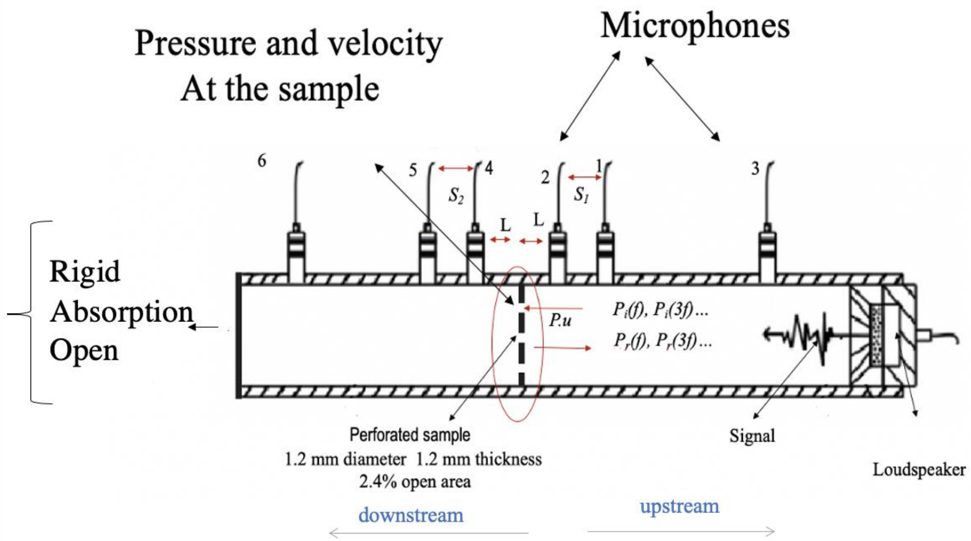

❖ Non-linear scattering matrix

$$\begin{pmatrix} p_r(f) \\ p_r(3f) \end{pmatrix} = \begin{bmatrix} S_{f,f} & S_{f,3f} \\ S_{3f,f} & S_{3f,3f} \end{bmatrix} \begin{pmatrix} p_i(f) \\ p_i(3f) \end{pmatrix}$$

$$p_r(f) = S_{f,f}\, p_i(f)$$

Indicator of the harmonic interaction

Inverse Strouhal number

❖ Incident acoustic velocity amplitude through the hole

$$\frac{1}{S} = \frac{u_{i,H}(f)}{\omega t}$$

- $u_{i,H}(f)$: Particle velocity
- ω : $2\pi f$ is the angular frequency
- t :Thickness

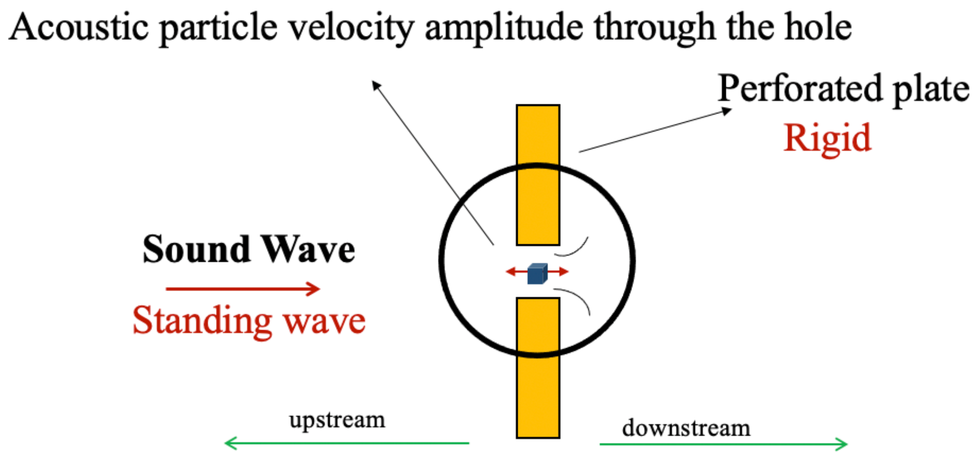

Results

ROYAL INSTITUTE OF TECHNOLOGY

Random

Abs($S_{3f,f}$)

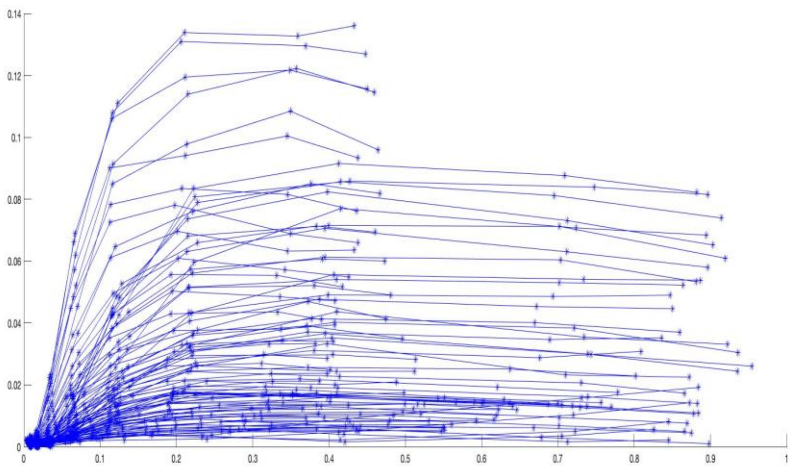

Fig. A

Inverse Strouhal number

Tonal

Abs($S_{3f,f}$)

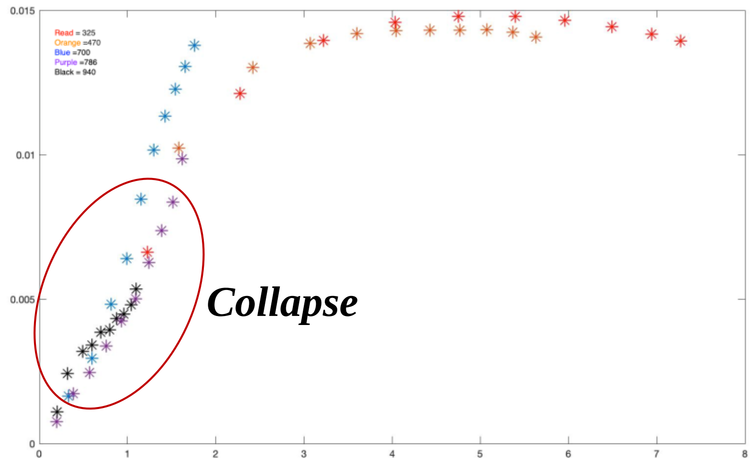

Fig. B

Inverse Strouhal number

N. khodashenas, H. Bodén, and S. Boij, Experimental study of nonlinear acoustic properties of perforates using band-limited random excitation information “. *Noise Control Eng. Euronoise 2018*, vol. 2, no. 43, pp. 1089–1096, 2018.

Bodén, Hans, Niloofar Sayyad Khodashenas, and Susann Boij. "Experimental study of nonlinear acoustic properties of perforates using band-limited random excitation information." 25th International Congress on Sound and Vibration 2018: Hiroshima Calling, ICSV 2018, Hiroshima, Japan, 8 July 2018 through 12 July 2018. Vol. 3. International Institute of Acoustics and Vibration, IIAV, 2018.

Smart ANSWER

Results

KTH VETENSKAP OCH KONST
ROYAL INSTITUTE OF TECHNOLOGY

Excitation frequency

Indicator of the harmonic interaction

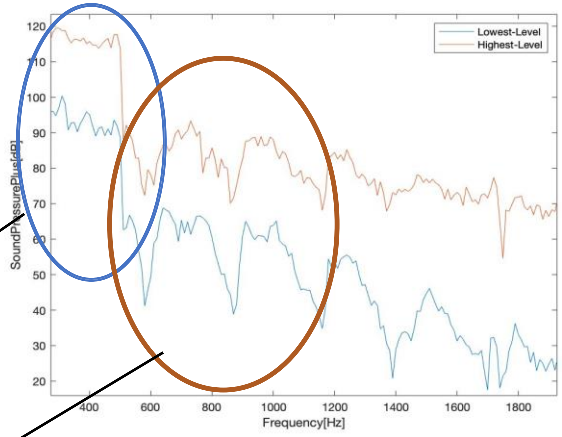

Fig. A

Random excitation

E- frequency

H-interaction

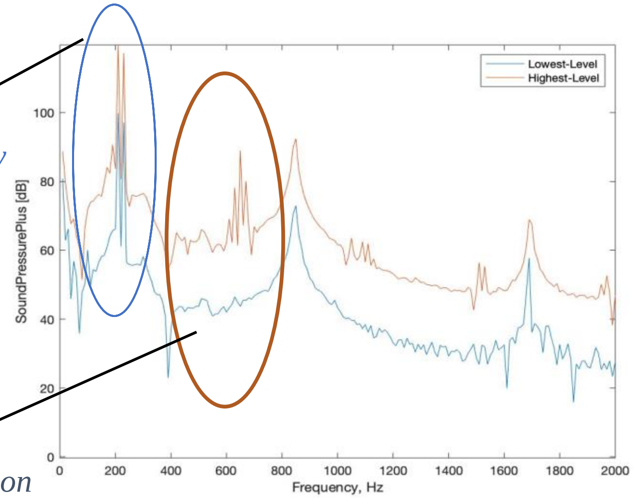

Fig. B

Two Tone excitation

E- frequency

H-interaction

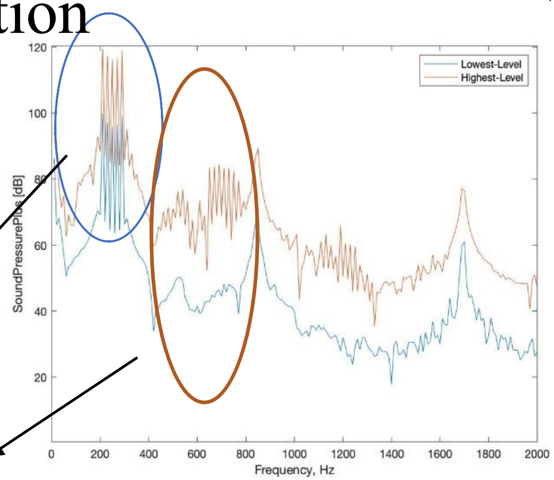

Fig. C

Five Tone excitation

Results

❖ Random excitation

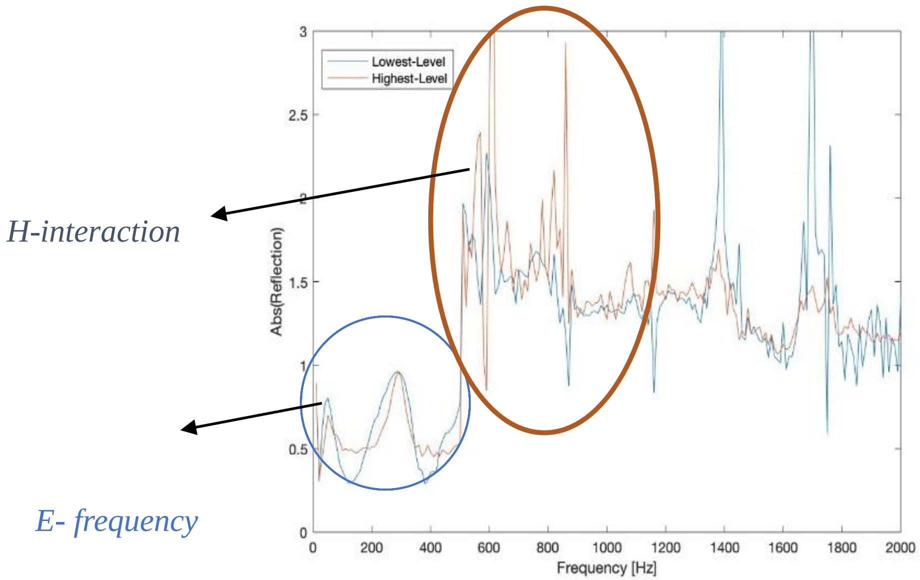

Fig. A

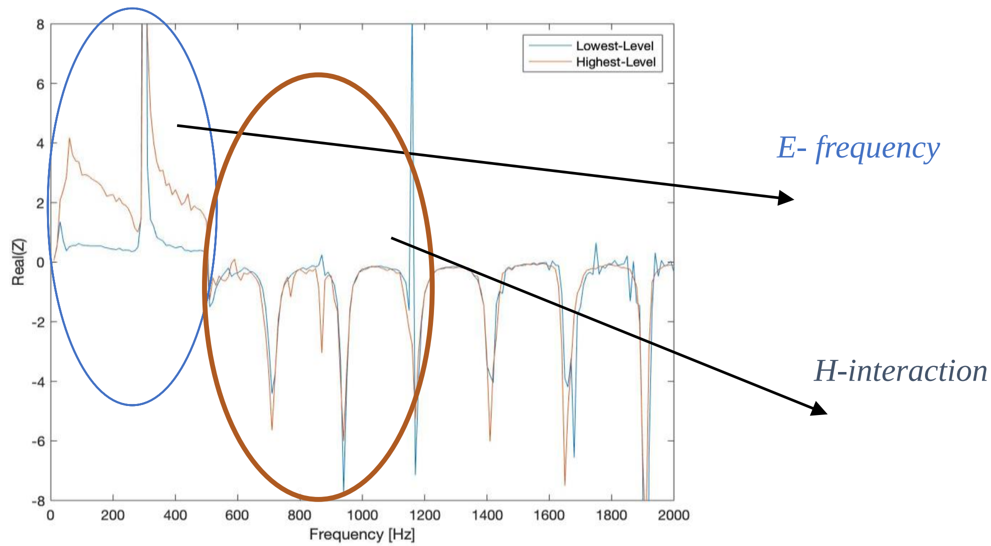

Fig. B

Real part of Reflection coefficient

Real part of the normalized impedance

Reflection factor

❖ Reflection factor in the excitation frequency range

$$R1 = \frac{\sum_{f=20}^{500} |p_r^u|^2}{\sum_{f=20}^{500} |p_i^u|^2}$$

❖ Reflection factor to the frequency range without excitation

$$R2 = \frac{\sum_{f=510}^{5000} |p_r^u|^2}{\sum_{f=20}^{500} |p_i^u|^2}$$

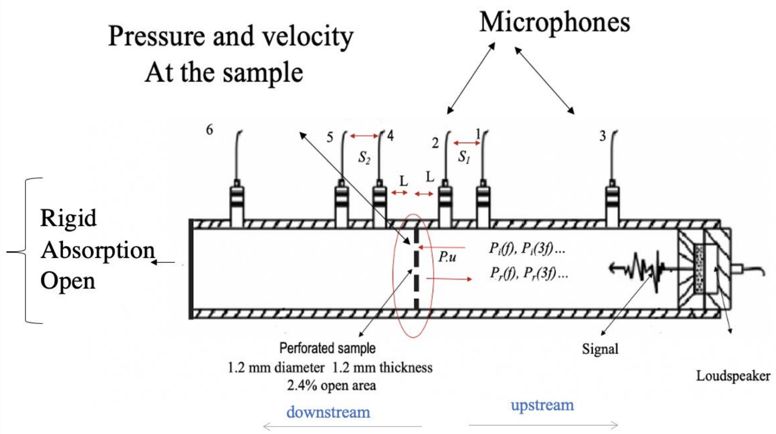

Transmission coefficient

❖ Transmission in the excitation frequency range

$$T1 = \frac{\sum_{f=20}^{500} \left| p_r^d \right|^2 - \sum_{f=20}^{500} \left| p_i^d \right|^2}{\sum_{f=20}^{5000} \left| p_i^u \right|^2}$$

❖ Transmission in the frequency range without excitation

$$T2 = \frac{\sum_{f=510}^{5000} \left| p_{\mathrm{r}}^d \right|^2 - \sum_{f=510}^{5000} \left| p_{\mathrm{i}}^d \right|^2}{\sum_{f=20}^{5000} \left| p_{\mathrm{i}}^u \right|^2}$$

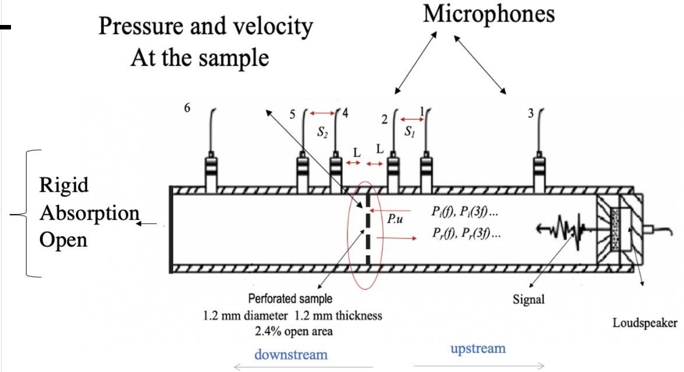

Absorption

❖ Absorption in the excitation frequency range

$$A1 = \frac{\sum_{f=20}^{500}|p_i^u|^2 - \sum_{f=20}^{500}|p_r^u|^2 + \sum_{f=20}^{500}\left|p_i^d\right|^2 - \sum_{f=20}^{500}\left|p_r^d\right|^2}{\sum_{f=20}^{500}\left|p_i^u\right|^2}$$

❖ Absorption in the frequency range without excitation

$$A2 = \frac{\sum_{f=510}^{5000}|p_i^u|^2 - \sum_{f=510}^{5000}|p_r^u|^2 + \sum_{f=510}^{5000}\left|p_i^d\right|^2 - \sum_{f=510}^{5000}\left|p_r^d\right|^2}{\sum_{f=20}^{500}\left|p_i^u\right|^2}$$

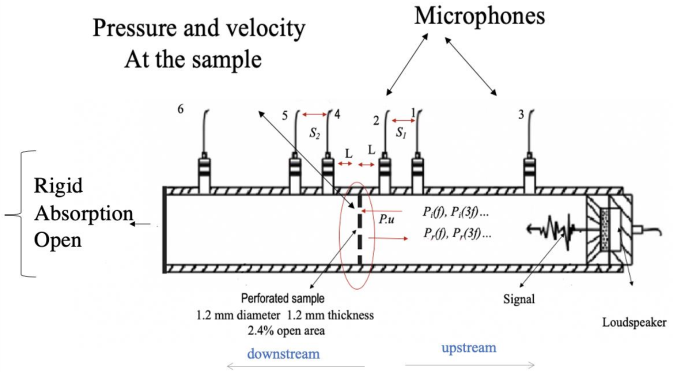

Results

ROYAL INSTITUTE OF TECHNOLOGY

Closed end downstream termination

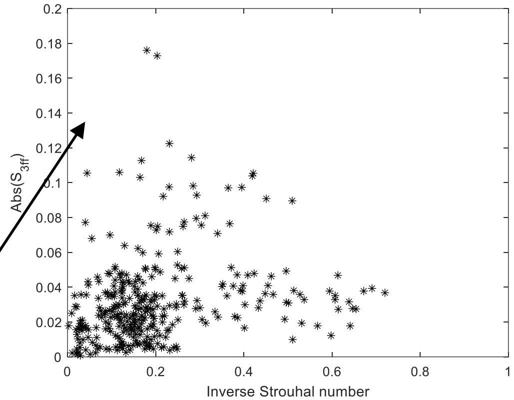

Fig. A (Random excitation)

Absorbing downstream termination

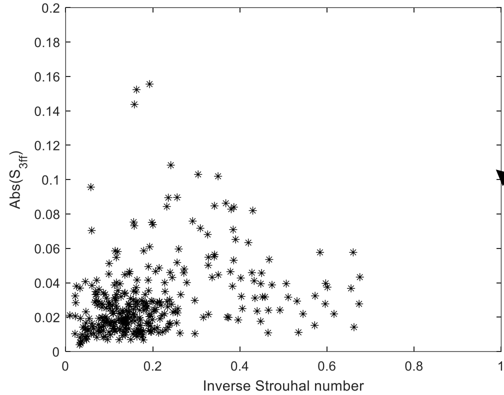

Fig. B (Random excitation)

Open downstream termination.

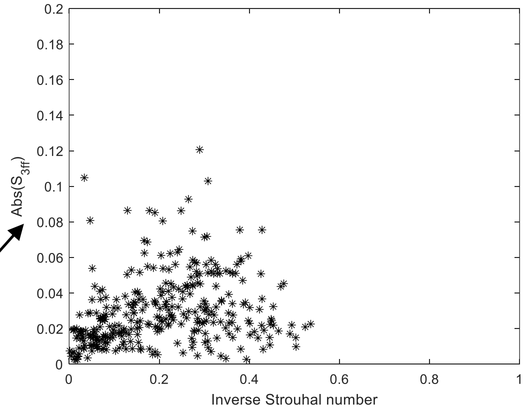

Fig. C (Random excitation)

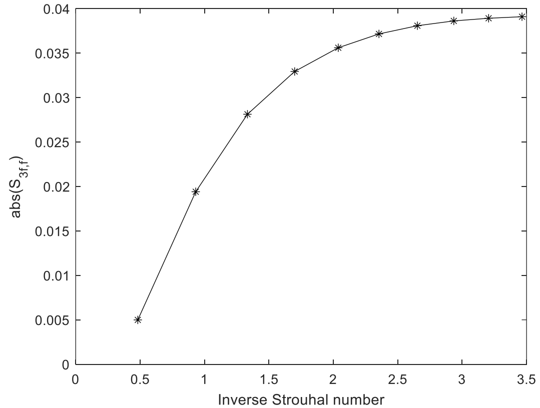

Fig. D (Tonal excitation)

Result

❖ **Absorption, Reflection, Transmission factor for Random excitation**

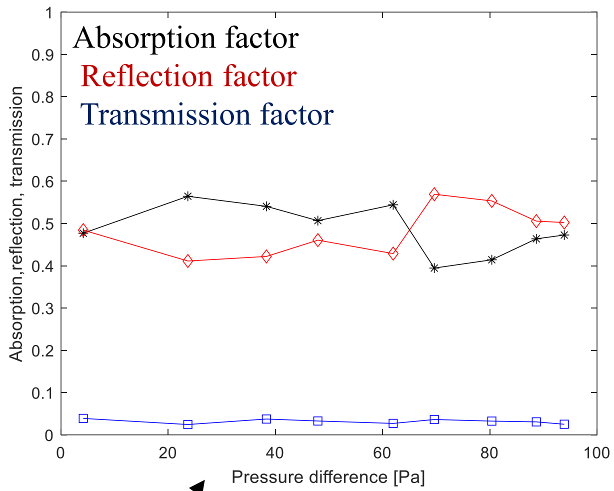

Fig. A

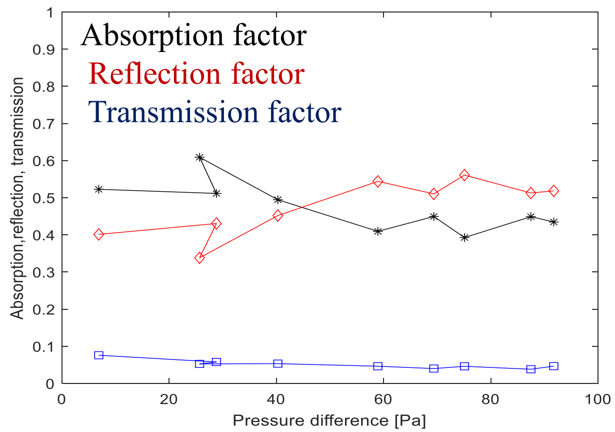

Fig. B

Absorbing downstream termination

Closed end downstream termination

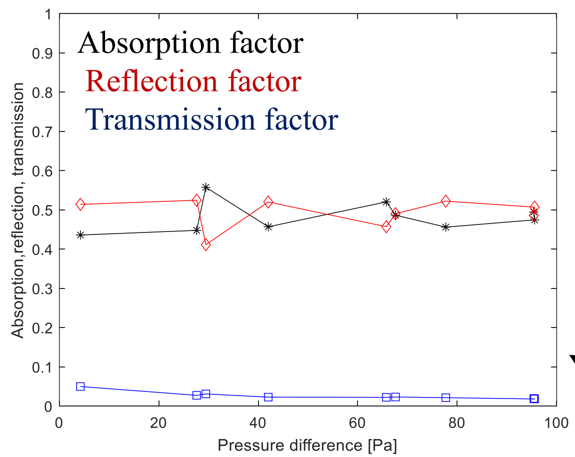

Fig. C

Open downstream termination

Result

- **Abs(S_{3ff})^2 ,and Reflection factor for Random excitation**

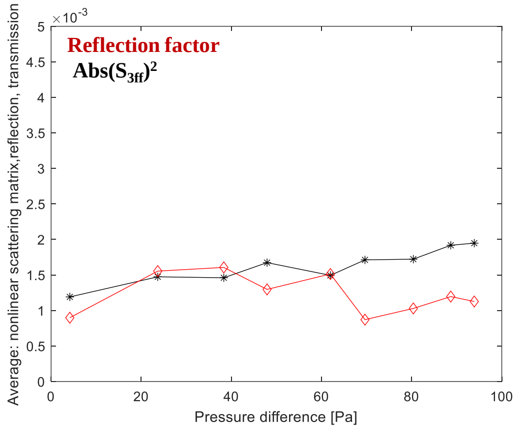

Fig. A

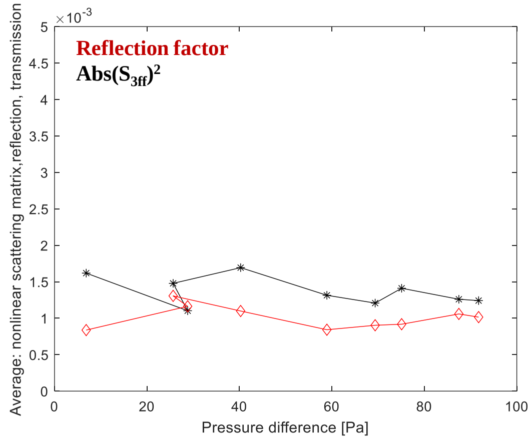

Fig. B

Absorbing downstream termination

Closed end downstream termination

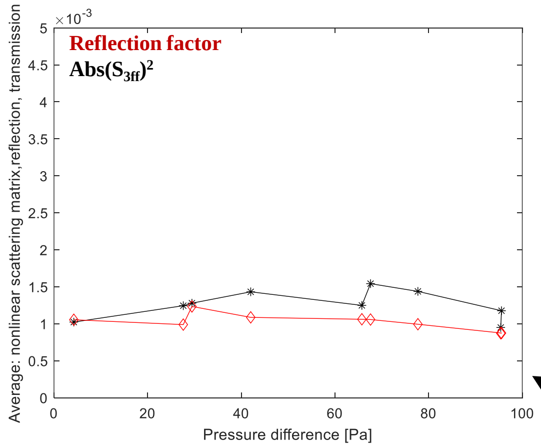

Fig. C

Open downstream termination

Khodashenas, N., H. Bodén, and S. Boij. "Determination of non-linear scattering matrices for perforated plates using tonal and random excitation." International Conference on Noise and Vibration Engineering. 2020.

Conclusions

- Non-linear scattering matrices will not work as already for multi-tone excitation the nonlinear transfer of energy to higher frequencies is not dominated by the odd higher harmonics alone.

- Averaged nonlinear scattering components and reflection factors over frequency bands seem to give consistent results and could be a way to quantify nonlinear interaction effects for multi-tone and random excitation.

- More Experiment and advance model

Smart ANSWER

HORIZON 2020 — THE FRAMEWORK PROGRAMME FOR RESEARCH AND INNOVATION

MARIE CURIE ACTIONS

Thank you for your attention

UNIVERSITY OF Southampton Institute of Sound and Vibration Research

von KARMAN INSTITUTE FOR FLUID DYNAMICS

KU LEUVEN

EPFL

TU Delft

National Technical University of Athens

CETIAT ensemble, innover et valider

IMP PAN GDAŃSK

ÉCOLE

LAUM

KTH VETENSKAP OCH KONST

Siemens PLM Software SIEMENS

SIEMENS Siemens Wind Power